بسم الله الرحمن الرحيم

A comparative study of intra-cavity photoacoustic resonances in a conventional and waveguide CO_2 lasers

By

Tayseer Mohammad Ibrahim Amro

B. Sc., Al-Quds University, Palestine

Supervisor: ***Dr. M. I. Abu- Taha***

Co – Supervisor: ***Dr. A. Leghrouz***

Thesis submitted in partial fulfillment of the requirements for the degree of Master of Physics

Physics Department, Al-Quds University

December 2001

Physics Master/Physics Department
Deanship of Graduate Studies

A comparative study of intra-cavity photoacoustic resonances in a conventional and waveguide CO_2 Lasers

Student Name: Tayseer Mohammad Ibrahim Amro

Registration No: 9720051

Supervisor: Dr. M. Abu-Taha

Co-Supervisor: Dr. A. Leghrouz

Master thesis submitted and accepted, date: 23/12/2001

The names and signatures of the examining committee are as follows:

1- Dr. M. Abu-Taha	Head of Committee	Signature .....
2- Dr. A. Leghrouz	Internal Examiner	Signature .....
3- Dr. Mustafa Abu-safa	External Examiner	Signature .....

Al-Quds University

2001

Declaration

I certify that this thesis submitted for the degree of Master of physics, is the result of my own research, except where otherwise acknowledged, and that this thesis (or any part of the same) has not been submitted for a higher degree to any other university or institution.

Signed.....

Tayseer Mohammad Ibrahim Amro

Date: 23/12/2001

Acknowledgements

It is great pleasure to acknowledge the contribution of people in the preparation of this thesis. My deepest thanks go to my supervisors Dr. M. Abu-Taha and Dr. A. Leghrouz for their interest, guidance, encouragement and valuable suggestions through the period of study.

I would also thanks my friend Dr. M. Abu-Sammrha for his help through numerous discussions.

Thanks also to Ahmad Amro (Abu Anass), Mr. Asad and Ahlam Amro for photographing and typing this thesis.

Finally I offer special thanks to my father, mother and to my Fiancee Areej Amro for their encouragement, forbearance during the preparation of this thesis.

Abstract

Carbon dioxide laser is famous by the large number of spot frequency lines it generates. Therefore this laser system has many applications, scientific, industrial, agricultural and medical. The laser is most useful when operated in a stabilized mode. The objective of this study is to compare PA signals detected in two types of the CO_2 laser carriedout by Abu-Taha, 1987 and Parslow, 1993. Data were derived from an experimental curves obtained by both researchers. Trials were also carriedout to calculate the theoretical resonances assuming the different formula for PA cell designs. A difficulty was encountered in deciding the exact volume of the cavity involved in the cell action. Similarity of curves shapes and approximate resonance values confirmed the PA signals were generated in the vicinity of the laser beam in the cavity and expanded into the rest of all parts connected to it. The PA signals are found to be a good indicator of the physical processes that takes place in the laser cavity. It seems that the PA signals are also generated in the discharge region of the laser. In general it can be said that the study showed an agreement between theoretical and experimental measured frequencies for both conventional and waveguide laser, although discrepancies exist within experimental errors and satisfaction of the acoustic cell conditions.

List of figures

List of tables

Contents

Chapter 1.

Introduction

1-1 Historical background

The word laser is an acronym for light amplification by stimulated emission of radiation. That radiation is in the form of photons of light, which is the end product of light amplification that is produced, in turn, by stimulated emission (Ratz, 1995). Several lasers were proposed from 1958 through 1960, however the first laser to emit coherent light was the ruby laser invented in 1960 by Maiman. The helium- neon- gas laser was developed by Javan, 1961, later a wide variety of lasers have been developed, and it can now be said that the era of the laser has come at last. Patel, 1964 developed the carbon dioxide laser. The 1980 began with a new surge in laser use and new functions were found for the available lasers. Technologic advances brought new laser systems and upgrades of older lasers and ancillary equipment that fostered an almost exponential growth of laser use in dermatology in the mid- to late 1980s and into the 1990s (Apfelberg, 1992). Lasers are designed in different types and shapes depending on the used active material. In the following a brief a count is given:

A- Gas lasers for example: Neutral atom lasers (He-Ne copper and gold vapor lasers), Ion lasers (Argon laser, He-Cd laser), molecular lasers (CO_2, CO, N_2 lasers).

B- Solid state lasers, for example: Ruby laser and, Neodymium lasers.

C- Liquid lasers, for example: (Dye laser).

D- Chemical lasers, for example: (The HF laser).

E- Semiconductor lasers, for example: (GaAs laser).

F- Color –center lasers, for example: (F_2^+center laser).

G- X–rays lasers.

H- The free- electron laser.

Lasers have found many applications, such as:

1- Industrial application in material processing, for example:

Welding, hole drilling, and cutting.

2- Laser in medicine: For example in surgery.

3- Laser in science: For example, harmonic Generation, self- focusing, and applications in chemistry and biology and many other scientific branches.

4- Lasers in communication. For example: Large information- carrying capacity of light waves, (Thyagarajan and Ghatak, 1981).

Laser system is mostly useful when operated in a stabilized mode. This can be a cheived using many techniques; for example the Photoacoustic (PA) and the optogalvanic (Abu-Taha, 1987) effects. Both effects depend

on the process being going on in the laser cavity. The Photoacoustic effect is the process of acoustic wave generation in a sample resulting from the absorption of photons. This Process was first discovered by Alexander Braham Bell in 1880, and before that Tyndall and Rontegen (1980) who had heard of Bell's discovery. Tyndall and Roentgen then work together on the same experirnents, in which optical radiation was chopped by passing it through a rotating slotted disk and then directing it into a closed chamber containing the sample. Before that nearly 50 years the photoacoustic effect revived again by development in microphone technology. This development encouraged Viengrov (1938) to use the phenomenon to study infrared light absorption in gaseous species in gas mixtures. A year later (Pfund, 1939) described a gas analyzer system for measuring the concentration of CO and CO_2. Significant step forward was achieved by (Luft, 1943). When he used gas analyses that employed two-photoacoustic cells. In 1946, Gorelik, first proposed a method of measuring the phase of the transfer between the vibrational and the transnational degrees of freedom of gas molecules using this technique. The next important step forward in the development of the photoacoustic effect was the first use of a laser as a radiation source by Kerr and Atwood (1968). They successfully in that year managed to measure the absorption spectrum of water vapor, and also the absorption spectrum of CO_2 and N_2. Since the 1970s, with the presence of the laser and the progress of highly sensitive

pressure detectors, the PA technique flourished and used in many applications. This thesis is concerned with a comparison study between results obtained for PA signals from both conventional and waveguide CO_2 laser cavities. Understanding of PA signals generated in the CO_2 laser cavity will result in good understanding of sustained stabilization and enhancement of laser power.

1-2 Thesis Plan

This thesis contains the following chapters:

a- Chapter one: This chapter introduces the CO_2 laser and brief study of the general types and applications of laser and the historical background to the photoacoustic technique.

b- Chapter two: Explains the properties of the CO_2 laser and brief description of excitation methods.

c- In chapter three a brief review of the photoacoustic technique is given.

d- Chapter four deals with the derived PA experimental results, accompanied by experimental description of the measurement techniques.

e- In chapter five results are analyzed and their indications of what is going on in the cavity is discussed.

f- The last chapter deals with conclusions and further suggested work.

Chapter 2

The carbon dioxide laser.

2-1 Introduction

For successful laser operation, four important conditions need to be satisfied. First, there must be an active medium, that is collection of atoms, molecules, or ions that emit radiation in the optical part of the electromagnetic spectrum of interest. Second, population inversion, a condition required for light amplification, it constitute an abnormal distribution of atoms among the various available energy levels. To understand how light amplification can be achieved in a medium, it is necessary to consider what constitutes a normal distribution of atomic-energy- state population, hence population inversion in a laser is created by an excitation process known as pumping. Third, feedback, for a true laser oscillation to take place, there must be some form of optical components present in the laser to supply feedback energy into the system. Finally, a suitable sources of energy that is necessary to supply the energy to the active medium (Bloom, 1968), in this chapter the necessary components and conditions for operating a CO_2 laser will be discussed.

2-2 CO_2 laser theory

2-2-1 The CO_2 laser

The CO_2 laser considered by some to be the most important molecular laser operated to date. The first molecular gas laser constructed by (Patel, 1964), with a few milli watts of power output. The wide range of applications of the CO_2 laser has made possible by the fact that it has the highest efficiency among industrial lasers, can be operated both in the pulsed and Cw mode, and can be tuned, albeit discretely, over the range 9.4μm and 10.4μm (Patel, 1968). The CO_2 laser has two properties, which distinguish it from other lasers (Tyte, 1970). Firstly, although it radiates in the mid- infrared, it's emission wavelengths lie in an atmospheric window, which means that CO_2 laser beam can be directed from point to point through the air using conventional optical methods. Secondly, due to the simplicity of the laser basics, it can be assembled using materials and techniques available in almost every physical science laboratory.

2-2-2 CO_2 molecule modes.

In general, the vibration of a polyatomic molecule is very complex but it can be considered as the sum of a number of simple vibrations. The CO_2 molecule is linear and symmetric in configuration with three degrees of vibrational freedom. For a molecule containing N atoms, each of these atoms can move in three perpendiculars, the sum of these individual

movements will be 3N degree of freedom. The center of gravity in all modes of vibration remains fixed. The CO_2 molecule was chosen to be the main component of the laser active medium for two reasons: -

1- The CO_2 is one of the simplest of the triatomic, and it has a quit well-known spectrum in the infrared region

2- The CO_2 is reactive, linear and has asymmetric arrangement of atoms.

The CO_2 molecules can oscillate in four degrees of vibrational freedom, But as illustrated in figure 2-1, two of these degrees correspond to the same vibrational mode, i.e bending mode.

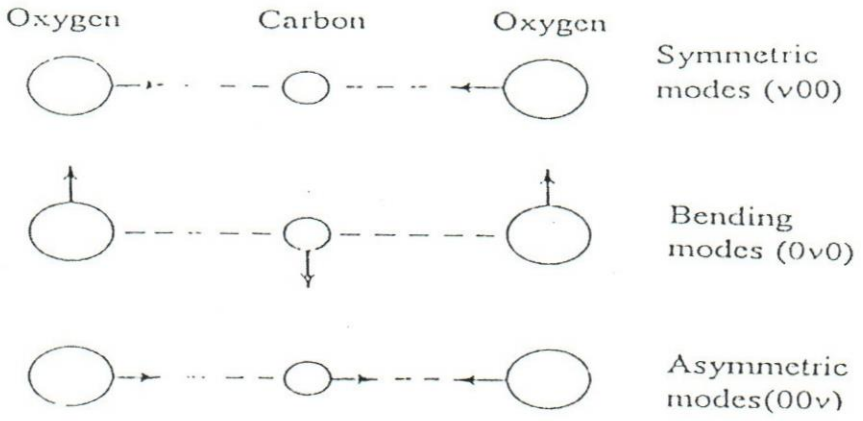

Fig 2-1 Normal vibrational modes of the CO_2 molecule

(After Scott, 1984)

The first of the three vibrational modes is the symmetric stretching, in which the center of gravity of the molecule remains fixed in all modes of vibration, this mode has a characteristic frequency denoted by ν_1. The second vibrational mode is called the bending mode, which consists of two degenerate vibrations, and the oxygen atoms oscillate perpendicularly to the internuclear axis. These two vibrations have the same energy and frequency, denoted by ν_2. Finally, the third mode is called asymmetric stretching mode, one bond is stretched while the other is compressed, and vices versa. This mode has a frequency denoted by ν_3.

2-2- 3 Energy levels of CO_2 molecules

The energy of oscillation of CO_2 molecule in any one mode can have only discreet values, just as the energy of electronic levels quantized. The state of the molecule can be described by CO_2 (n_1, n_2, n_3) where n_1 describes the number of vibration quanta in the symmetric stretching mode, n_2 the number of vibrational quanta in the bending mode and n_3 the number of vibrational quanta in the asymmetric stretching mode.

The symbol ℓ which simply characterize the combinations, takes on the values:

$\ell = n_2, n_2 - 2, \ldots, 0$- for even n_2.

$\ell = n_2, n_2 - 1, \ldots, 1$- for odd n_2.

For addition, this symbol determines the angular momentum ℓth of this vibration about the axis of the CO_2 molecule. This indicates that when $n_2 = 1$ the possible value of ℓ is equal to 1, but when $n_2 = 2$ the possible value of ℓ can take two values, namely $\ell = 2$ or $\ell = 0$. The levels are denoted by the form $(01^1 0)$ and $(02^2 0)$, respectively (Duley, 1976).

The bending frequency ν_2 is 667 cm^{-1} where as the stretching frequency (ν_1 and ν_2) are 1340 cm^{-1} and 2349 cm^{-1} where ν_2 energy can be achieved from a transition $(00^0 0)$ to the upper laser level $(00^0 1)$, (Richard's and Scott, 1985). As can be seen from, figure (2-2) the bending ν_2 achieved from a transition $(01^1 0)$ to upper level $(02^0 0)$ and like that ν_1 (Sobolov, 1967). Rotational states (R) associated with rotation of the molecule about the center of mass are also possible. The separations between vibrational, and rotational states are usually much smaller on the energy stack than separations between electronic states, the rotational energy is also quantized. Thus, the energy levels of the rotational modes can be calculated by the equation (Svelto, 1989):

$$E_r = hc\, BJ\,(J+1) \ldots\ldots\ldots (1)$$

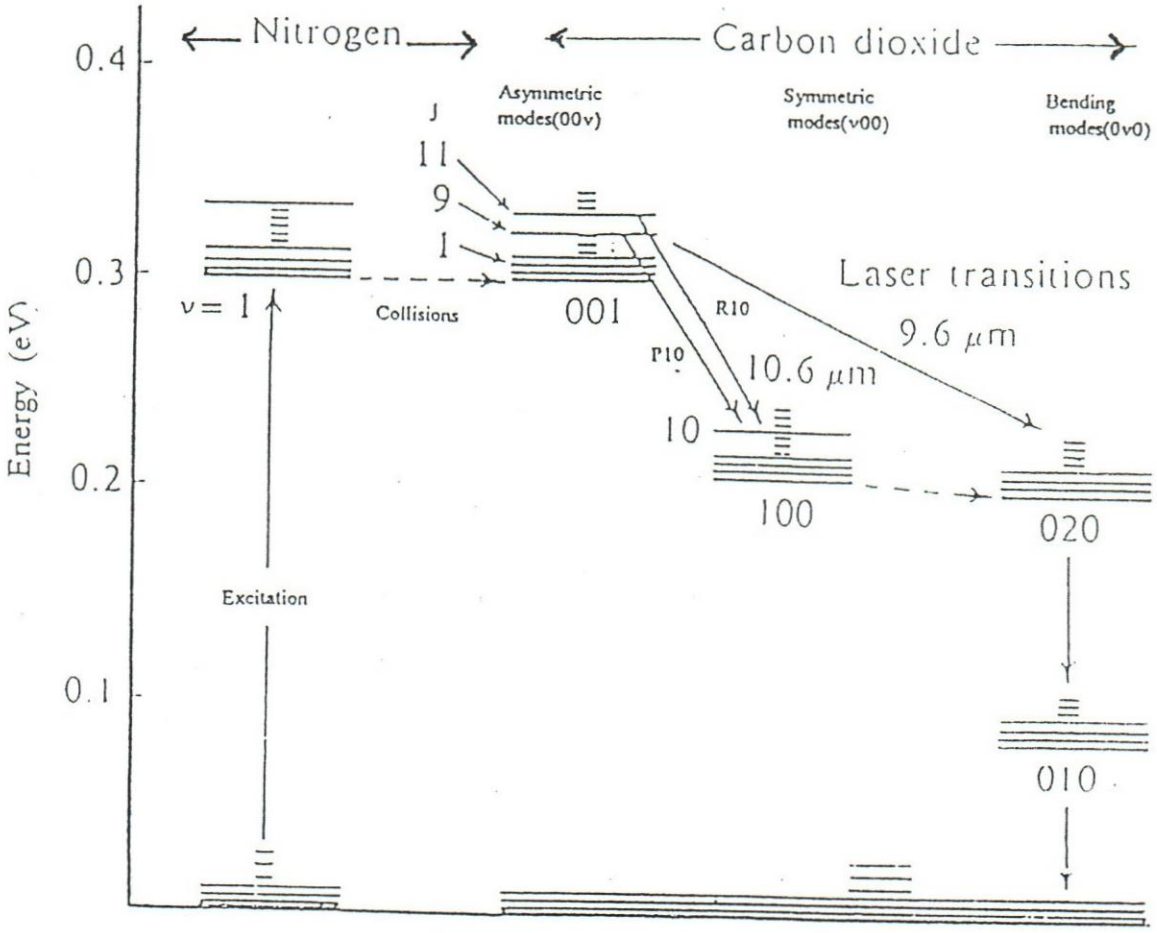

Fig 2-2 Energy level diagram of the CO_2 and N_2 molecules.

(After wood, 1974)

Where B is the rotational constant equal to ($h/ 8\pi^2cI$), I the moment of inertia given as $I = \mu r_o^2$, r_o is the bond length, μ is the reduced mass and h is Planck's constant, c is the speed of light and J is the rotational quantum number, which can change by ±1. According to equation (1) the value of J may be zero or any positive integer. When the population of the upper laser level (001) exceeds that of the (10̊0) level and population inversion takes place, the downward transition between these level should obey the selection rule, (i.e J can only change by ±1). Thus if J = 20 for certain level, then the two possible transition are J = 18 → 19 and J = 19→ J = 20. When J change by (+1) the transition is that of the P- branch, contrary when J change by (-1) it is named as one of the R- branch transition. The transition from J = 19 to J = 20 is written as P20, and that from J = 21 to J = 20 as R20 as shown in figure (2- 3).

In summary the selection rule for vibrational – rotational transitions between energy levels are as follows: -

$\Delta n = 0$, no change in vibrational state.

$\Delta J = 0$, no change in rotation spectra.

$\Delta n = \pm 1$, transition between vibrational levels.

$\Delta J = \pm 1$, transition between rotational states.

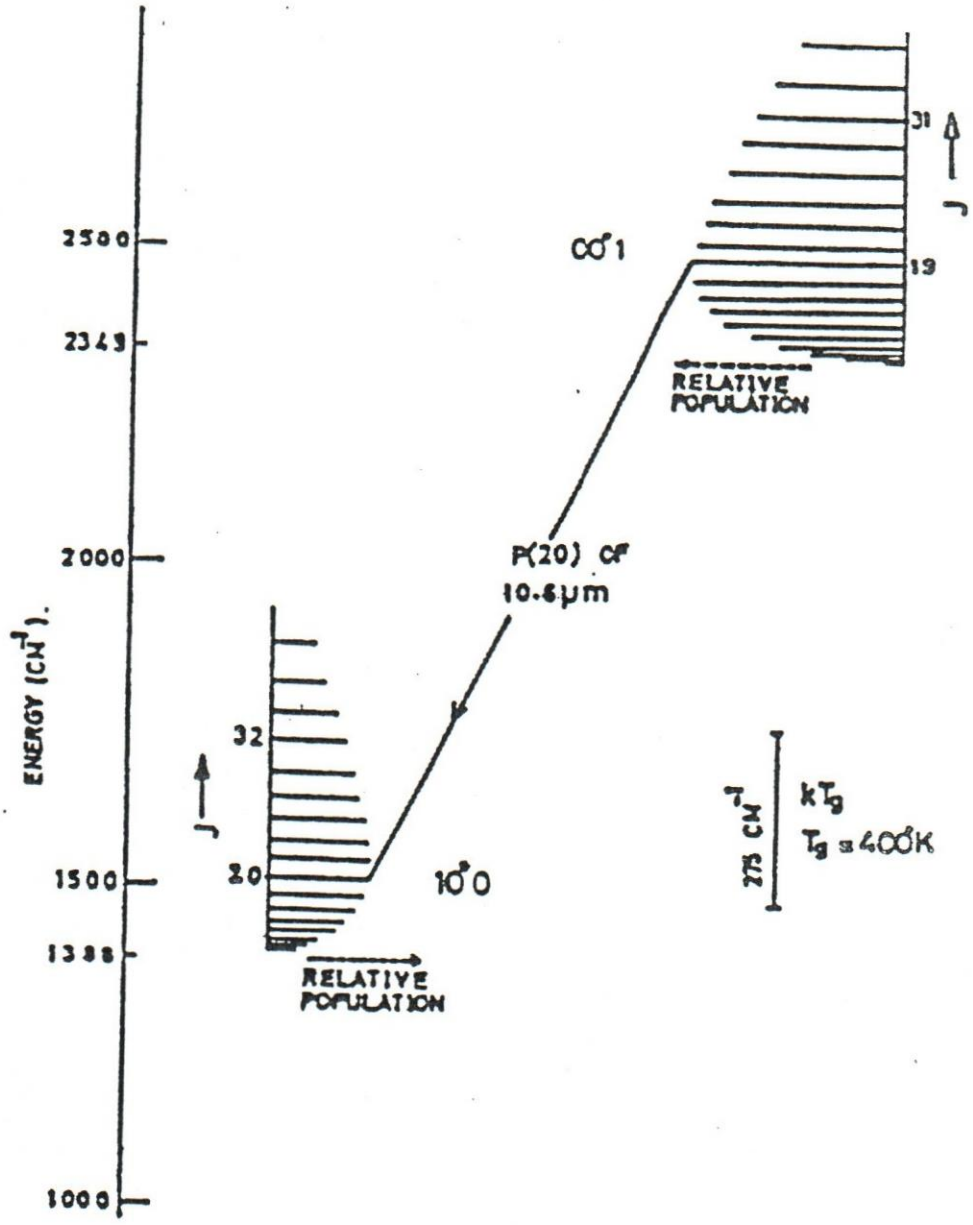

Fig 2.3 Sub- rotational levels populations of upper and lower laser levels

(After Tychinskii, 1967)

If we have no transition between vibrational states, which possess the same J value that is called the Q branch. The transition is from asymmetric (odd ^{+}J) to symmetric (even ^{+}J) only, (Lengyel, 1971). Since the spacing of these rotational energy level is smaller than the kinetic energy of the molecules, (which is about 0.to 0.25ev at room temperature), the molecule can jump around from one rotational level to another very frequently.

Further, since the CO_2 molecule has a center of symmetry and the spins of the oxygen nuclei, are zero, the negative rotational levels are missing. Thus for the electronic ground state the molecules with symmetric vibrational levels have only even J numbers in the rotational spectrum, while only odd J number exist for the anti symmetric vibrational levels. For an equilibrium distribution, the Jth rotational energy level is given by Boltzman distribution, and is determined by formula (Manes et al. 1972):

$$n_J = N_v(2J+1)\frac{hcB}{kT_g}\exp\left[\frac{-Er}{KJgas}\right] \quad \text{.....(2)}$$

Where n_J is the rotational level under consideration of thermal equilibrium Nv the total population of the vibrational level (v), h is the Planck's constant, c is the speed of light, k is Boltzman constant and T_g is the gas temperature in degrees Kelvin.

Assuming J to be a continuos variable and differentiating equation (2) with respect to it, and setting the resulting equation equal to zero, it can be

shown that the quantum number of the rotational level with the greatest population is: -

$$J_{\max} = \sqrt{\frac{KT_{gas}}{2hcB}} - \frac{1}{2} \approx 0.95\sqrt{T_{gas}} - \frac{1}{2} \quad \text{.....(3)}$$

For $T_g = 400K$, $B = 38.66\ m^{-1}$ then $J_{max} = 19$ that cheived for (00^01) level as figure 2- 3 shows (Tychinskii, 1967).

2-3 vibrational relaxation times

A measure of the probability of transition is the level lifetime τ, it is considered to be either the period of time over which the transition takes place (i,e., the period of time over which the quantum of energy, hν, is absorbed or released), or equivalently, it is the period of time during which the solution to the schroedinger equation can applied. Since the atomic system may remain in the upper state of forbidden transition for thousand to million times longer than in the upper state of an allowed transition, the upper states of forbidden transition are referred to as a metastable state.

The relaxation time (τ_{AB}) associated with transfer of energy between the symmetric stretching mode and the bending mode of CO_2 molecule is given by (Manes et at, 1972) by the equation: -

$$\tau_{AB} = \frac{1}{N_{CO_2} D_{AB}} \left[\frac{\exp(h\nu_B / KT_B) - 1}{\exp(h\nu_B / KT_B) + 1} \right] \quad \text{.....(4)}$$

where τ_{AB} is the relaxation time associated with the transfer of energy between the CO_2 symmetric stretching mode and the bending modes, D_{AB} is a constant, T_B is the effective temperature of CO_2 bending mode, $h\nu_B$ the quantum of energy of the bending mode, N_{CO2} the number of CO_2 molecule and K thermal conductivity of the gas.

The relaxation time of the anti symmetric mode, τ_C is given by the following equation:

$$\tau_c(T, T_A, T_B) = \frac{\left[\exp\left(\frac{h\nu_A}{kT_A} \right) - 1 \right] \left[\exp \frac{(h\nu_B}{KT_B} - 1 \right]}{\left[N_{CO_2} D_C (\exp\left(\frac{h\nu_A}{kT_A} + \frac{h\nu_B}{KT_B} + \frac{h\nu c - h\nu_B - h\nu_A}{KT} \right) \right]} \quad \text{.....(5)}$$

where D_C is constant, T_A the effective temperature of the CO_2 anti symmetric stretching mode $h\nu_A$, $h\nu_B$, $h\nu_C$, the quantum energy of one symmetric mode, bending mode and anti symmetric stretching mode, respectively.

Taylor and Bitterman, (1969) described a relation from the different relaxation times that can be obtained as a function of temperature and pressure of the different CO_2 gas mixtures: -

$$\tau_{ij}(T) = [N_{CO2} \, Kij_{CO2}(T) + N_{N2} \, Kij_{N2}(T) + N_{He} \, Kij_{He}(T)] \quad \text{.....(6)}$$

where Kij is called the kinetic rate constant, which its values are given for various ij values by (Manes et al, 1972), N_{N2} the number of N_2 molecule/ $cm^3$and N_{He} the number of He atom / cm^3.

The experimental value of life times to the transition of CO_2 (00^01) to (10^00) gave values of (0.93± 0.05) ms and (90 ± 20) ms respectively, (Crafer, Gibson, Kent and kimmit, 1969). Tychinskii (1967) estimated these values of lifetime of the order of 1ms and 0.3 ms respectively. Crafer et al (1969) found that the addition of helium gas does not change the measured value of the (00^01) level life time significantly and that the N_2 – CO_2 transfer time was about 0.3 ms. Flynn and Javan (1966) found that molecules in the level (00^01) could be lost by collisions with the other excited molecules CO_2 (00^01) or excited N_2 (n =1) and the result led to the formation of excited CO_2 $(00n_3)$. Sobolov et al. (1967) Found the time in which the (00^01) level could be excited again after it was depleted was of the order of 10^{-15} second. At P_{CO2} = 1torr and operation at room temperature, the $CO_2 - CO_2$ (pure gas) collision cross section is nearly 1.6 $x10^{-15}$ cm^2 (Sobolov et al, 1967). At least 5×10^2 collisions of molecules in the CO_2 (10^00) level with other molecules were needed to transfer these to the (01^10) level. It was concluded from the measured collision rate at one torr pressure of CO_2 at room temperature, that molecules themselves are the main agents of the relaxation process from the lower laser level. It was necessary for the (01^10) level to be depleted effectively, other wise a

decrease in the population inversion occurred as CO_2 molecules were expected to accumulate in this level (Patel, 1968). The life time of this level was determined using the formula (Sobolov et al, 1967):

$$\frac{1}{\tau 01^{1}0} = \frac{P_{CO2}}{\tau_{CO2\,-CO2}} + \frac{P_{tot} - P_{CO2}}{\tau_{CO2-\mu}} \quad \text{.....(7)}$$

where $\tau_{CO2\text{-}\ CO2}$: the relaxation time as a result of collision of CO_2– CO_2 molecules, $\tau_{CO2\,\text{-}\mu}$: the relaxation time as a result of collision of a CO_2 molecule and an atom in the discharge. P_{tot} , the total pressures of two molecule (CO_2 and N_2) which given by

$P_{tot} = P_{CO2} + P_{\mu}$ or $P_{CO2} + P_{N2}$..... (8)

The relaxation of CO_2 ($00^{0}0$) states occurs through

$CO_2\ (01^{1}0) + M \rightarrow CO_2\ (00^{0}0) + M + 667cm^{-1}$ ..... (9)

Where M could be CO_2 molecule.

Figure (2-4) shows the relaxation times of continuous wave CO_2 laser operation at 15 torr and at temperature of 420 kelvin.

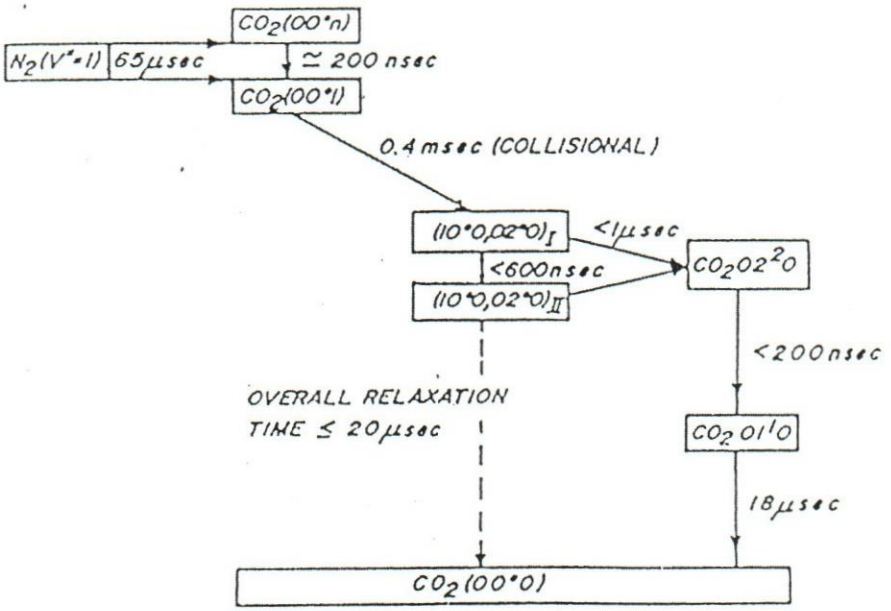

Figure: 2-4 Relaxation times in a continuous wave CO_2 laser at 15 torr and 420K (After Tyte, 1970).

2-4 Laser operation

2-4 –1 Laser operation with pure CO_2 gas.

The most important condition for laser operation is the attainment of population inversion. In the CO_2 laser a condition of population inversion between the transition (00^01) and (10^00) emitting at range ($\lambda = 10.6\ \mu$ m) or in the (00^01) and (02^00) emitting at ($\lambda = 9.4\mu$m). It is usually the transition (00^01) and (10^00) that oscillates, more ever the level (10^00) has the greater collision cross section and both transition share the same upper level (00^01), (Svelto, 1989).

Pumping of the upper laser level can be achieved by: -

Direct electron collisions: -

The main direct collision to be considered is: -

$e + CO_2 (00^0 0) \rightarrow e + CO_2 (00^0 1)$ ..... (10)

This process also leads to the excitation of upper vibrational level (00n) of the CO_2 molecule, which relaxes rapidly from the upper states to the (001) state by near – resonant collisions for $n > 1$.

$CO_2 (00n) + CO_2 (00^0 0) \rightarrow CO_2 (0, 0, n - 1) + CO_2 (00^0 1)$ ..... (11)

It should be mentioned that this process continues until all the excited molecules are degraded to the $(00^0 1)$ state (Svelto, 1989). It is not possible to rely on such a process for laser operation hence the use of N_2.

N_2-CO_2 collision:

This is very efficient process since the energy difference between the excited level in CO_2 and N_2 is small ($\Delta E = 18\ cm^{-1}$). This process is represented by the equation (Duley, 1976): -

$N_2 (n = 1) + CO_2 (00^0 0) \rightarrow N_2 (n = 0) + CO_2 (00^0 1) - 18cm^{-1}$ ..... (12).

In addition for the higher vibrational levels of (00n) of the CO_2 molecule, the higher vibrational levels of N_2 are nearly of equal separation. Thus, these two sets of vibrational levels are separated to make an excellent match with one another up to the (008) vibrational level. Therefor, efficient transitions between the excited (00n) levels, with $n \leq 8$ and the $(00^0 1)$ level

of the CO_2 molecule occur rapidly as described by the process in equation12.

2-4- 2 Laser operation with gas mixture.

In order to achieve an extremely high continuous output power, with high efficiency it is necessary to use additional gases such as N_2, He, water vapor, hydrogen and other gases in the discharge tube. These gases can increase the rate of de–excitation of the lower vibrational levels of the CO_2 molecules as well as increasing the rate which CO_2 molecules are excited to the (001) level. N_2 and He are of special importance in CO_2 laser systems, although other gases can be added. In the following brief discussion of gases that can be added to CO_2 laser system.

Nitrogen (N_2)

Nitrogen in the CO_2 laser plays a similar role to that of helium in the He-Ne laser. Nitrogen is a diatomic molecule with one degree of freedom and with zero dipole moment. Since the first excited vibrational level of N_2 is only slightly below the highest energy level of the CO_2 molecule, ($\Delta E = 18$ cm^{-1}), the excited N_2 molecules can transfer their energy to the CO_2 ($00^0 0$) molecules through resonant collisions, exciting them to the ($00^0 1$) level. Further more, nitrogen reduce the lifetime of the lower laser level. (Tychinskii, 1967) found that if P_{N2} =1torr, N_2 (n =1) has lifetime about 14.5-16ms,which indicates that this molecule a metastable has the first

excited vibrational state. The importance of N_2 in enhancing output power has been confirmed experimentally by many researchers. For example, (Howe, 1965) found that the power output could be increased by a factor of three if nitrogen was added to laser active medium.

Helium (He)

Moeller and Rigden, 1965 discovered that the addition of helium to the carbon dioxide and nitrogen mixture would result in an increase in the population of the upper laser level as will as decrease in the population of the lower laser level. In flowing gas system, it is found that a CO_2–N_2–He mixture produces more power (about four times) than with a CO_2–N_2 combination. Helium has a very good thermal conductivity (k) compared with other gases. Tychinskii, 1967 reported the following values for thermal conductivity of laser gas mixture:

$K_{He} = 0.344 \times 10^{-3}\ wk^{-1}\ S^{-1}$.

$K_{N2} = 0.057 \times 10^{-3}\ wk^{-1}\ S^{-1}$.

$K_{CO2} = 0.03 \times 10^{-3}\ wk^{-1}\ S^{-1}$.

With high thermal conductivity helium helps to keep the carbon dioxide cool by conducting heat away to the container walls. The electrical discharge heat will cause temperature difference between the gas and the wall of the tube. This temperature difference is inversely proportional to the thermal conductivity of the gas. The role of the gas will increase the

thermal conductivity to the walls of the tube resulting in decrease of the gas temperature, this results increasing the gain. The best result was obtained with all three mixed together at the following pressures 2. 7 torr CO_2, 7.8 torr He and 3. 5 torr N_2 (Moeller and Rigden, 1965). A near subtle role for He is relaxing the lower laser level. Since the first excited state of He occurs at 159. 850 cm^{-1}, the (00^01) level is not affected when He is added to the CO_2–N_2 mixture (Verdeyen, 1995). It was found that such collisions, i.e. He-CO_2 can take place at rate of 4000 collisions persecond at a pressure of 1 torr (Patel, 1968).

Water Vapor

The addition of small amount of H_2O vapor increase the out put power by a factor of at least two (Witteman, 1966). At higher pressure that 0.25 torr, H_2O proved to be harmful to laser operation (Smith, 1969). The addition of water vapor to a mixture containing CO_2 and N_2 gases will increase the rate of de-excitation of the (100) level. Due to the vibration angle between the two O-H bonds in the H_2O molecules, the corresponding lowest vibrational frequency of this molecule is 1596 cm^{-1}. This frequency is close to that of the symmetrical vibration of CO_2, the energy of this molecule by relatively few collisions. Moreover, through collisions with H_2O molecules the deactivation of the vibrational energy of the H_2O is very rapid (Witteman, 1966).

Carbon monoxide (CO)

Carbon monoxide plays the same role as N_2, but the efficiency of CO is lower than N_2. CO decrease the possibility of CO_2 excitation (Smith, 1969).

Oxygen (O_2)

The addition of O_2 gas to CO_2 was not helpful, on the other hand, a pressure of 0.1 torr of O_2 will result in a reduction in the laser power output between 10-15%. This result was obtained by (Howe, 1965) who reported reduction of output power one half after adding O_2. Other information, oxygen excites CO_2 to the (10^00) and (02^00) levels and therefor reduces the population inversion. At an oxygen with pressure of 1 torr the O_2 (n = 1) relaxation time is equal to 2. 4 seconds (Tychiskii, 1967).

Xenon (Xe)

Xenon (Xe) has an effect of decreasing the electron temperature (Woods, 1974). Some of the above mentioned gases have, an effect on the relaxation life time of the CO_2 laser levels.

2-5 Energy level population

The population inversion required for light amplification constitutes an abnormal distribution of atoms among the various available energy levels. Boltzman principle specifies what fraction of atoms are found, on the average, in any particular energy state for any given equilibrium temperature given by (Duley, 1976):

$$N_b = N_a \exp[-E_b / KT] \quad \text{.....(13)}$$

Where: N_b is the number of atoms in the excited state, N_a is the number of atoms in the ground state, E_b is the excited state energy measured relative to the ground state energy, T is the absolute temperature in degrees Kelvin and K is Boltzman's constant equal to 1.38×10^{-23} Joule/ K. The ratio of the atomic populations in the gas for two arbitrary energy levels, $E_b > E_a$, for example, is easily shown to be: -

$$N_b = N_a \exp\left(\frac{-\Delta E_{ba}}{KT}\right) \quad \text{.....(14)}$$

A two-level system is a system in which atoms or molecules have only two electronic energy levels as shown in figure (2-5). When $\Delta E << KT$ the high temperature causes, the Boltzmann ratio to be near unity and the population at energy level E_a is nearly equal to the population energy level E_b, such a ratio occurs when $\Delta E = KT$, or equivalently, when the frequency of the transition obtained by the equation

$h\nu_{ab} = E_b - E_a = KT$ ..... (15)

where h is the Planck's constant, since by equation (13) when $E_b > E_a$, N_a is always greater than and at absolute zero all the atoms or molecules

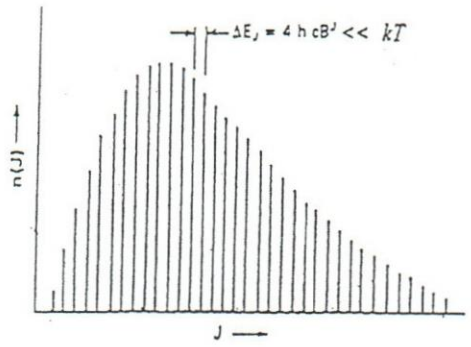

Figure 2-5 Boltzmann distribution of the population among the rotational levels of the upper laser level (for which only odd J values are permissible) (After Biswas et al, 1990)

will be in the lowest energy level (a) (Duley, 1976). It is found that: -

1- The rate of transition of atoms or molecules from (a) level was given by:

$R_1 = B_{ab} N_a \rho(\nu_{ab})$..... (16)

Where $\rho(\nu_{ab})$ is the energy density at the resonant frequency (J/ m^3HZ).

B_{ab} is the Einstein coefficient, which is a measure of the strength of (a) to (b) transition (m^3/ J^2).

2- The rate of transition of molecules from level (b) to (a) can be given by:

$R_2 = B_{ab} N_b \rho(\nu_{ab})$..... (17)

At equilibrium $B_{ab} = B_{ba} = B$.

In an applied electromagnetic field, molecules in level (b) can spontaneously emit a quantum of energy $h\nu_{ab}$ to drop to level (a). The rate of this spontaneous decay is given by: -

$R_3 = N_b A_{ba}$ ..... (18)

Where: $A_{ba} = (8\pi\ h\nu ab^3/\ c^3)$ B. A_{ba} is the Einstein coefficient with unit (sec^{-1})., and c is the speed of light. Since the system comprises two energy levels then:

$R_1 = R_2 + R_3$ ..... (19)

To obtain a system in which the stimulated emission is larger R_1 then N_b must be greater than Na (population inversion) between the two levels. $\rho(\nu ab)$ must be as large as possible to allow full use of population inversion (Duley, 1976). It was found that to have a population inversion, N_b must be greater than N_a to have a system acting as an amplifier for radiation of frequency $\nu_{ab} = (E_b - Ea/\ h)$.

In figure (2-6), the electrical discharge excites N_2 molecules to establish a population in an energy level (1). Practically, the only way for de-excitation of N_2 is by energy transfer to state (2) of CO_2 molecules.

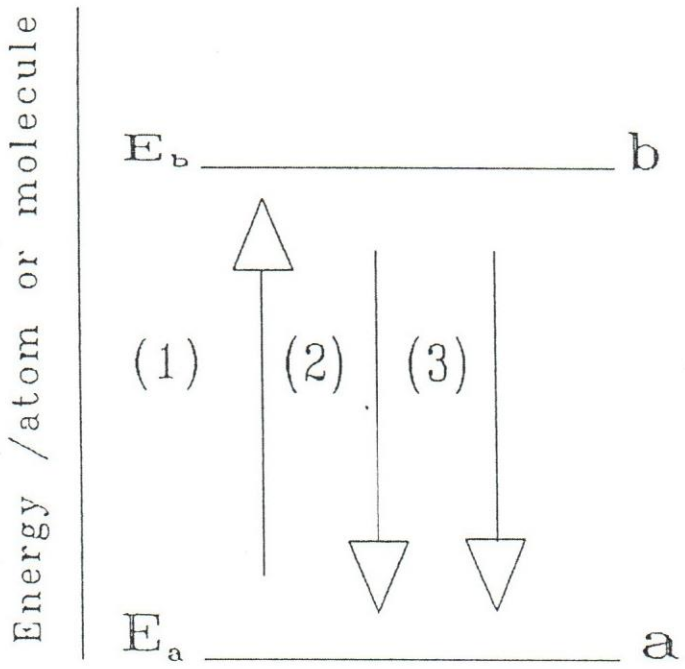

Figure 2-6 Two- levels system interacting with electromagnetic radiation of frequency (After Scott, 1984)

This causes the colliding CO_2 molecule to be raised from its ground state (o) to the excited state (2). A population inversion can be built up between levels (2) and (3). The population decay through stimulated emission from (2) to (3) results in the transfer of population to level (3), and for efficient operation some method must be provided for returning the molecules in this level to the ground state, other wise the population build up in level (3) will reduce the inversion between levels (2) and (3). When adding helium gas and some other gases to the gas mixture in the CO_2 wave guide laser tube, then population buildup is strengthened in (2) and weakened in (3), as

mentioned before in section (2- 6). The laser action in the system is controlled by collisional activation and deactivation rates and does not rely on radiative processes; a wide variety of parameters (gas pressure, composition, temperature, discharge current, electron temperature) has its effect on the CO_2 laser system.

2.6 Types of CO_2 laser

2-6-1 Conventional CO_2 lasers

Conventional CO_2 lasers can be separated into six types: -

a) Laser with lows axial flow or conventional CW CO_2 laser.

The operation of the first CO_2 laser was achieved in a laser of this type (Patel, 1964). The gas mixture is slowly flowed along the laser tube as shown in (figure 2-7).

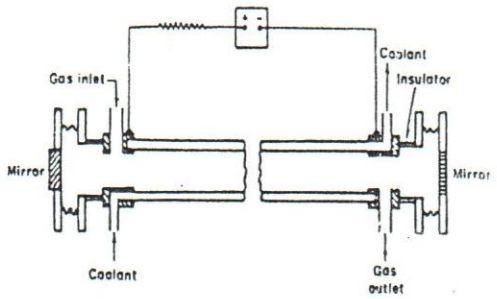

Figure 2-7 Schematic diagram of a CO_2 laser with longitudinal gas flow. (After Svelto, 1989).

Heat removal is provided by radial conduction of heat to the tube walls made of glass, which are cooled externally by a suitable coolant. One of the main limitations of this laser arises from the fact that there is a

maximum laser output power per unit length of the discharge (50- 60w/m) that can be obtained, independent of the tube diameter. This fact can be seen in the following way. For a given current density J, the number of molecules pumped into the upper laser level per unit time can be written as:

$$\left(\frac{dN_2}{dt}\right)_p \cong \frac{J\sigma_e N_g}{e}\left(\frac{v_{th}}{v_{drift}}\right) \quad \text{.....(20)}$$

where σ_e is a suitable electron–impact cross section, N_g is the total CO_2 ground population, e is the electron charge, ν_{th} is the thermal velocity and ν_{drift} is the drift velocity.

For pump rates above threshold, the output power, P, is proportional to (dN_2 / dt) and P that can be written as:

$$P \alpha J N_g V_a \alpha J_p D^2 L \quad \text{..... (21)}$$

Where: V_a is the volume of the active material in the laser tube having a diameter D, length L and P the output power.

For optimum operating conditions the following must be met:

1- The product PD must be constant to keep the discharge at optimum electron temperature.

2- Because of thermal limitation arising from the requirement of heat conduction to the tube walls, an optimum value of the current density exists, and this value is inversely proportional to the laser tube diameter D (Svelto, 1989).

b) Laser with fast axial flow

For the above type of CO_2 laser to overcome the output limitations, one possible solution and a particully very interesting one is to flow the gas mixture through the tube at very high supersonic speed (about 50 m/s). When operated in this way there is no optimum value for the current density, the power actually increases linearly with J, and much higher out put power per unit discharge length can be obtained nearly one kW/ m or greater. Besides cooling, the mixture, while it is outside the laser tube, also passed through catalyst to let CO react with O_2 (some O_2 is already present in the mixture owing to dissociation of the CO_2 in the discharge region). This provides for the required regeneration of CO_2 molecules.

Fast axial flow CO_2 lasers with high power between 1- 3 kW are used for material working applications and in particular for laser cutting of metal for a thickness up to a few mm.

(c) Sealed- off laser:

This type of laser can be achieved if the flow of the gas mixture were stopped in the arrangement as figure (2-8), laser action would cease in a few minutes. For a sealed- off laser, some kind of catalyst must be present in the gas tube to promote the regeneration of CO_2 from the CO. A simple way to achieve this is to add a small amount of water 1% to the gas mixture. This lead to regeneration of CO_2, probably through the reaction

$$CO\ (excited) + OH \rightarrow CO_2\ (excited) + H \quad \ldots\ldots\ldots\ldots (22)$$

The relatively small amount of H_2O vapor required may be added in the from of hydrogen and oxygen gas, another way of inducing the recombination reaction relies on the use of a hot (300°c) Ni cathode, which acts as a catalyst. The output powers of sealed-off lasers are nearly 60W/ m, comparable to those for longitudinal flow lasers. Lower power nearly 1w sealed off lasers of short length and hence operating in a single mode are often used as local oscillators in optical heterodyne experiments. Sealed- off CO_2 lasers of somewhat higher power nearly (10W) are attractive for laser microsurgery and for micromachining.

(d) Transverse – flow lasers

The power limitation of a low axial flow laser is to flow the gas mixture perpendicular to the discharge as fig (2- 8).

If the flow is fast enough, the heat, as in the case of fast axial flow lasers, gets carried away by convection rather than by diffusion to the walls, as in the case of fast axial flow, very high out put powers per unit discharge length can be obtained a few kW/m. It should be obtained, at pressures nearly 100 Torr. The increase in total pressure P requires a corresponding increase of the electric field in the discharge.

To attain the operating condition, the ratio E/P must remain approximately the same for all these cases determined the average energy of the discharge electrons.

The transverse electric field CO_2 lasers with fast transverse flow and high out put power (1- 20 kW) are used in a great variety of metal- working applications (cutting, welding, surface hardening, surface metal alloying). Compared to the fast axial flow lasers, these lasers appears to be simpler devices in view of the reduced flow speed requirement for transverse rather than axial flow.

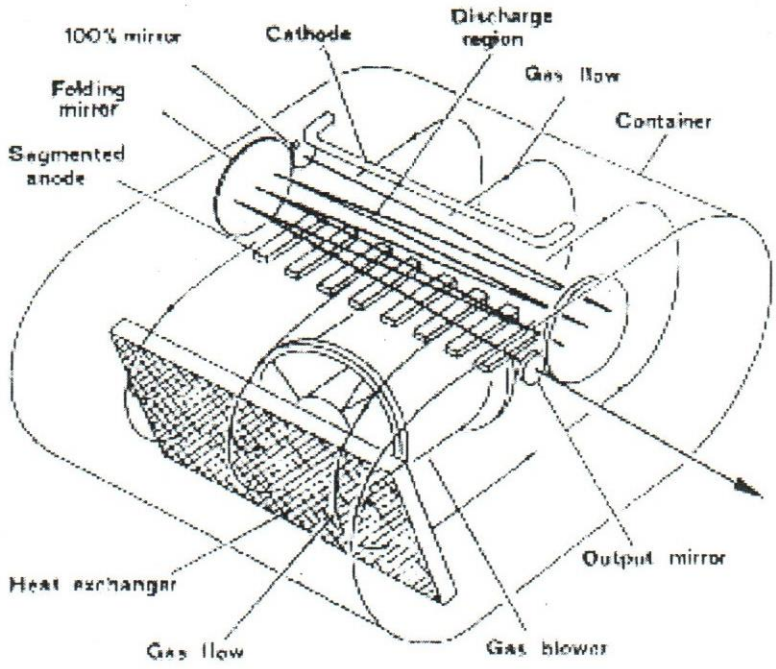

Fig: 2-8 Diagram of a particularly simple transverse- flow CO_2 laser. (After Svelto, 1989).

(e) Transversely excited atmospheric (TEA) lasers

These types of lasers are called TEA; the abbreviations standing for transversely excited at atmospheric pressure. It is not easy to increase the

operating pressure above nearly 100 torr, in a CW TEA CO_2 laser. Above this pressure and at the current densities normally used, glow discharge instabilities set in and result in the formation of arcs within the discharge volume. The voltage can be applied to the transverse electrodes in the from of a pulse. If the pulse duration is sufficiently short (a fraction of a microsecond), the discharge instabilities have no time to develop and the operating pressure can than be increased up to and above atmospheric pressure.

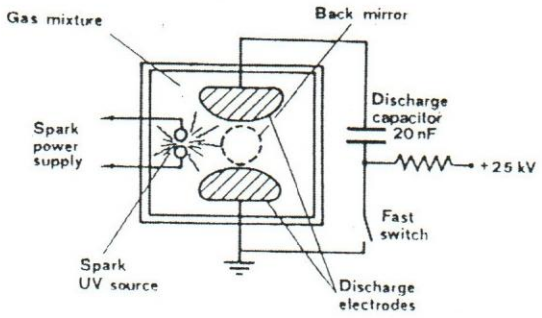

Fig 2-9 Schematic diagram (viewed along the laser axis) of a laser pumped by a transverse discharge using UV radiation from a spark source to preionize the gas. (After Svelto, 1989).

These types of lasers produce large output energies per unit volume of the discharges (10-50J/liter) as shown in figure (2-9). For low pulses (nearly 1Hz), it proves unnecessary to flow the gas mixture. On the other hand for higher repetition rate greater than few kilohertz the gas mixture is

flowed transversely to the resonator axis and is cooled by a suitable heat exchange. Another interesting characteristic of these laser is their relatively broad line widths nearly 4 GHz at P = 1 atm, due to collision broadening). TEA CO_2 lasers, are used in scientific application, find a number of industrial uses for those material working applications in which the pulsed nature of the beam presents some advantage (Svelto, 1989).

(f) Gas - Dynamic laser.

In the gas-dynamic CO_2 laser, population inversion is not produced by an electrical discharge but by rapid expansion of a gas mixture, which has initially been heated to a high temperature. Population inversion is produced downstream in the expansion region. Gas-dynamic CO_2 lasers have produced some of the largest powers so far reported in the unclassified literature. The operation principle of a gas- dynamic laser can be summarized as follows in figure (2-10 a). Since the gas is initially in thermal equilibrium and at a high temperature, the population of the $00^0 1$ level of CO_2 will be appreciable nearly 10% of the ground- state population as figure (2-10b). The lower- level population is of course, higher than this nearly 25%, and there is no population inversion. Now suppose the mixture is made to expand through some expansion nozzles as figure (2-10 c). Since the expansion is adiabatic, the transnational temperature of the mixture will be reduced too much lower value. Gas- dynamic CO_2 lasers have been reported that produce out put power up to 80 kW with chemical

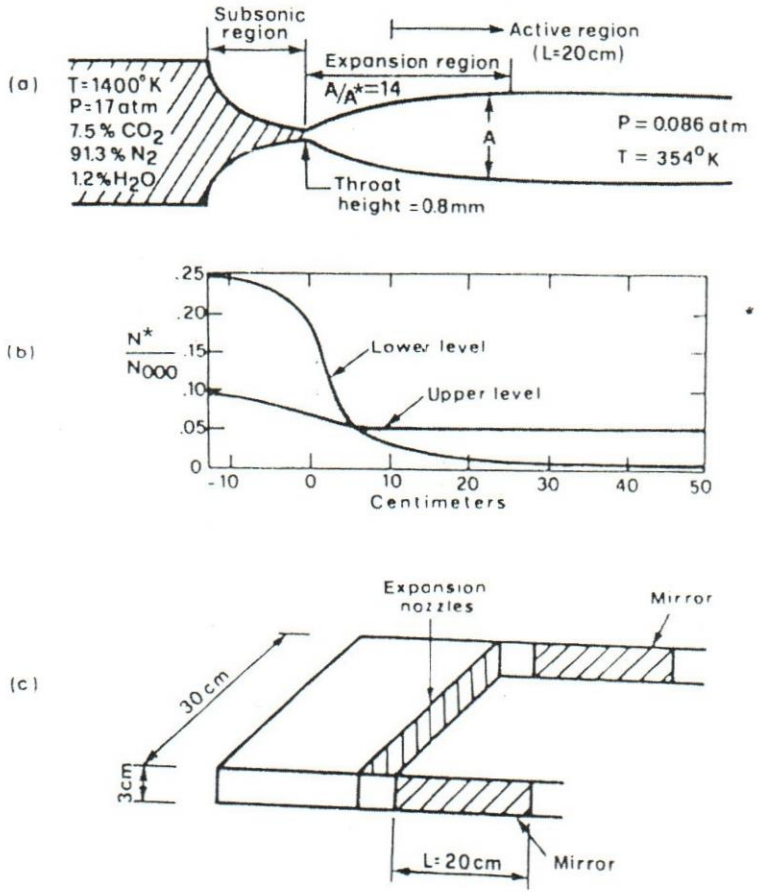

Fig 2-10: Schematic illustration of the operation of gas- dynamic CO_2 laser (a) principle of the system. (b) Spatial behavior of the population N^* for the upper and lower laser levels (c) cavity geometry (After Svelto, 1989)

efficiency of 1%. Continuous operation from such a laser has only been produced for a short time (a few second) because of the heating produced by the laser beam in some of the components (particularly the mirrors). Finally, the applications of gas dynamic lasers have not yet been found. Our brief mention made here has been to emphasize the conceptual interest of creating a population inversion by a gas- dynamic expansion.

2.6-2 Waveguide CO_2 laser

The waveguide laser is defined as a wave guided laser beam. Light waves are guided in part or across all of the laser waveguide. The first idea of the wave-guide laser was suggested by (Marcatili and Schmiltzer, 1964), a waveguide laser is a laser that employ a wave-guide resonator to provide the necessary year feed back to establish oscillation (Abrams, 1979). Marcatili and Schmiltzer investigated to the modes of hollow dielectric guides and compared between the guide's diameter, width to the wavelength of the light. After the work of Marcatili and Schmeltzer, Steffen and Kneubuhl, 1968 utilized waveguiding concepts to explain the apparently anomalous explanation by (Marcatili et al, 1967) or transverse mode frequencies in a laser operation in the far infrared portion of the spectrum. Smith, 1971 reported the first actually designed waveguide laser.

The application of the wave guiding principle to CW CO_2 laser demonstrated by (Bridges, Burkhardt, Smith, 1972). They used direct current discharge excitation to the gain medium, and a flowing gas mixture of CO_2-N_2-He in a 1mm diameter, 30 cm long glass capillary tube. If the diameter of laser tube is in the range of 2-4 mm, then the inner walls of the tube guide the laser radiation. The use of such a narrow- bore laser gas discharge tube minimizes radiation diffraction losses and permits an increase in the pressure of the gas mixture (100-200 torr), as described by (Wilson and Hankes, 1987). If the length of CO_2 laser designed is less than 50cm without suffering cavity losses, the light pressure operation leads to an increase in laser gain per unit length, (Selvto, 1989). Line tunability and single mode operation of these short and compact low power ($P < 30W$) CO_2 lasers makes them very useful in spectroscopy and microsurgery.

Waveguide CO_2 lasers are widely used in research and industrial applications due to relatively high output power for their small size. As these lasers operate at a gas pressure of few hundred torrs, they have the potential of several MHz frequency determines from the line centers, (Pisarchik, kuntsevich, 1998). Powerful tunable coherent radiation sources are the mid- infrared region and especially valuable for power demanding applications such as optical pumping of molecular far-infrared lasers (Douglas, Millimeter and Submillimetre, 1989), photoacoustic (Olafsson, Henningsen, 1995), and photo thermal spectroscopy.

Hollow dielectric waveguide modes

A waveguide laser may be distinguished from a conventional one by the fact that over some portion of the propagation path, the circulating radiation is guided by the waveguide for at least some distance in the laser cavity. Cavity mode is defined as a field distribution that reproduces itself in relative shape and in relative phase after around trip through the system (Verdeyen, 1995). Marcatili and Schmeltzer, 1964, described the modes of propagation and their losses for hollow circular guides, and showed that there are three types of modes: -

1- Transverse circular electric modes (TE_{OM}), whose electric field is the first order tangential to the waveguide (wg) surface.

2- Transverse circular magnetic modes (TM_{OM}), whose magnetic field is the first order tangential to the (wg) surface.

3- Hybrid modes (EHnm) which have both components of electric and magnetic fields, where n is a positive integer describing the rotational symmetry of the field distribution, and m is a positive integer represents the number of maxim a and minim a in the field along the radial direction between r = o and r = a.

The electric field patterns of the lowest- order mode of each type are shown in figure (2-11).

If (wg) radius is much larger than the free space wavelength λ, the field distribution can be described as:

$Ka \gg |\mu| U_{nm}$ .....(24)

Where: $K = 2\pi/\lambda$ is the propagation constant of free space, a is the radius of the capillary tube, μ is the refractive index of the dielectric wall, U_{nm} is the m^{th} root of the equation $J_{n-1}(U_{nm}) = 0$ where J_n is the Bessel function with root n m is integers that identify the mode. The propagation constant for various modes can be calculated from the equation:

$$\gamma = K\left[1 - \frac{1}{2}\left(\frac{U_{nm}}{Ka}\right)^2\left(1 - \frac{2i\mu_n}{Ka}\right)\right] \quad \text{.....(25)}$$

Where the constant μ_n depends on the type of mode and the refractive index of the guide wall as shown below: -

$$\mu_n = \frac{\mu^2}{\sqrt{\mu^2 - 1}} \quad \text{.....} for TM om \bmod es (n = 0).$$

or

$$\mu_n = \frac{\mu^2 + 1}{\sqrt{\mu^2 - 1}} \quad \text{.....} for EHnm \bmod es (n \neq 0).$$

The real part of γ in equation (25) represents the phase constant β_{nm} and the attenuation coefficient α_{nm} can be obtained, respectively, as

$$\beta_{nm} = RE(\gamma) = K\left[1 - \frac{1}{2}\left(\frac{U_{nm}}{Ka}\right)^2\left(1 + \frac{2}{ka}\mathrm{Im}\right)(\mu_n)\right] \quad \text{.....(26)}$$

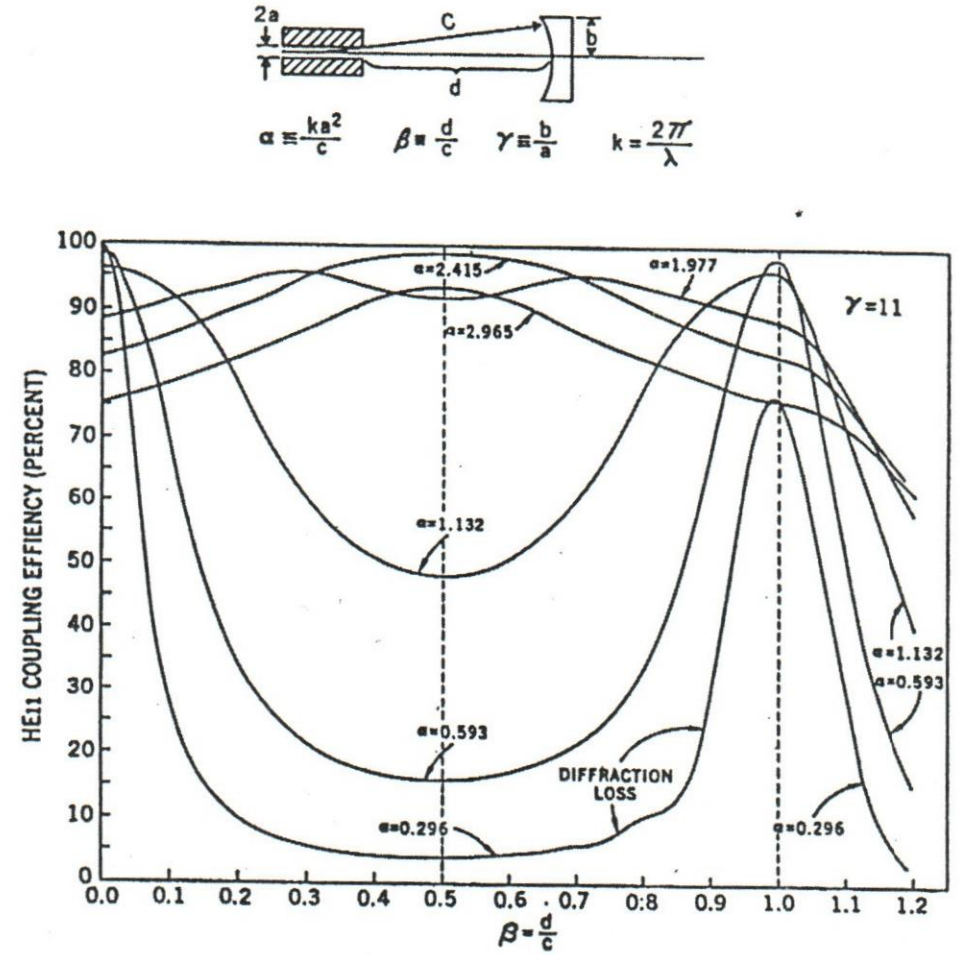

Fig 2-11: EH_{11} coupling loss as a function of guide and mirror parameters (After Degnan and Hall, 1976).

TE_{OM} – Circular electric

$$E_\theta = J_1\left(\frac{U_{om}}{a}\right)$$

$$E_r = 0$$

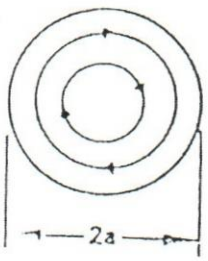

TM_{OM} – Circular Magnetic

$$E_\theta = 0$$

$$E_r = J_1\left(\frac{U_{om}}{a} r\right)$$

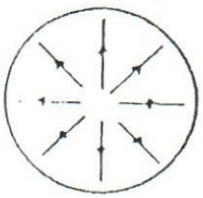

EH_{nm} – Hybrid Modes

$$E_r = J_{n-1}\left(\frac{U_{nm} r}{a}\right)$$

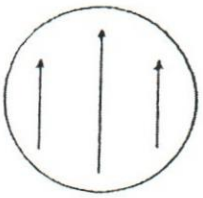

Figure (2-12): Analytic expression and characteristic electric field patterns for wave guide modes (After Abrams and Chester, 1972).

The propagation constant for the various modes is given by:

$$\alpha_{nm} = \mathrm{Im}(\gamma) = \left(\frac{U_{nm}}{K}\right)^2 \frac{\lambda^2}{a^3} \mathrm{Re}(\mu_n) \quad \text{.....(27)}$$

For equation (27) α_{nm} is proportional to λ^2 / a^3, hence losses can be minimized by making a »λ. Also, for a losses dielectric wall material, U_{nm}

Figure (2-14) is atypical circuit, which could be used to pass a DC current through a discharge used for a CW gas laser. In some cases the cathode is heated and supplies electron by thermonic emission while in others it is cold.

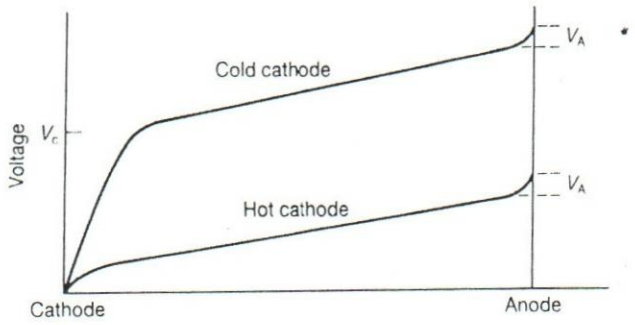

Fig 2-14 Variation of voltage between cathode and anode for a hot and a cold cathode discharge. (After Hawkes, Latimer, 1995).

The distinction between the two is illustrated if we plot the variation of the voltage between cathode and anode as shown in figure (2-14) we see from this figure that the cold cathode has a very much larger voltage drop at the cathode than does the hot cathode. The mechanisms at the cathode are complex but it is sufficient to state that this large voltage drop at the cathode accelerates the positive ions to produce electrons by positive ion bombardment. The supply of electrons at the cathode must balance those lost at the anode and so maintain current continuity in the circuit. The hot cathode, on the other hand, provides a copious supply of electrons and does

not require such a large voltage drop. Cold and hot cathode discharge have negative current voltage characteristics giving the circuit a negative dynamic impedance and the series- positive resistor is necessary to prevent relaxation oscillations of the circuit. The transistors are placed in series to proof amplitude stabilization of the discharge current and the gain. The material of the cold cathode usually made of hollow cylinder of aluminum on the other hand the hot cathode usually made of tungsten filament. A small voltage drop at the anode exists that accelerates electrons, resulting in heat and, as a consequence with high current discharges anodes must be cooled. Electrons are being produced in these collisions by ionization but at the same time are diffusing to walls where they are lost by recombination with the positive ions. This statement is called the Schottky theory, measures the rate of ionization, evaluated with the excitation cross-section replaced by the ionization cross–section, to the diffusive loss obtained from known measured diffusion coefficients (Cherrington, 1979). The assumption made in this theory is that the ion mean–free path is less than the tube radius. The discharge current has no effect on the electron temperature but changes the electron density in direction proportion. A further result of this diffusion theory is that the electron density varies across the tube diameter as a zero–order Bessel function, resulting in a radial gain variation which follows the same function. In a low–pressure discharge through narrow–bore tubes the ion mean-free path can be larger

than the bore of the tube and the electrons can fall freely without collisions to the tube walls. This is known as the Tonks-Langmuir regime and although the magnitudes are different the electron temperature is again found to be a decreasing function of the product pressure **x** diameter.

2-8 The Optical resonator

The optical resonator can be described as two mirrors or a mirror and optical grating arranged so that light is reflected from one to another. This assumption plays an important role in CO_2 laser performance since it effects the radiation distribution in the active medium and hence the out put beam quality. The amplification of an optical beam passing once through the active medium is usually minimal because the gain of a pumped or excited medium is very small 10% per meter, (Wilson and Hawkes, 1987). This amplification can be increased by using two highly reflecting mirrors facing each other and separated by a distance L that should be 10^5 times. The optical resonator can be divided into two types:

Stable and unstable resonators,some examples are shown in figure (2-15). In stable resonators the laser radiation is confined within the medium and the out put beam is transmitted through one or both mirrors, on the other hand in unstable resonators laser radiation suffers divergence, since it is not focused to remain within the active medium.

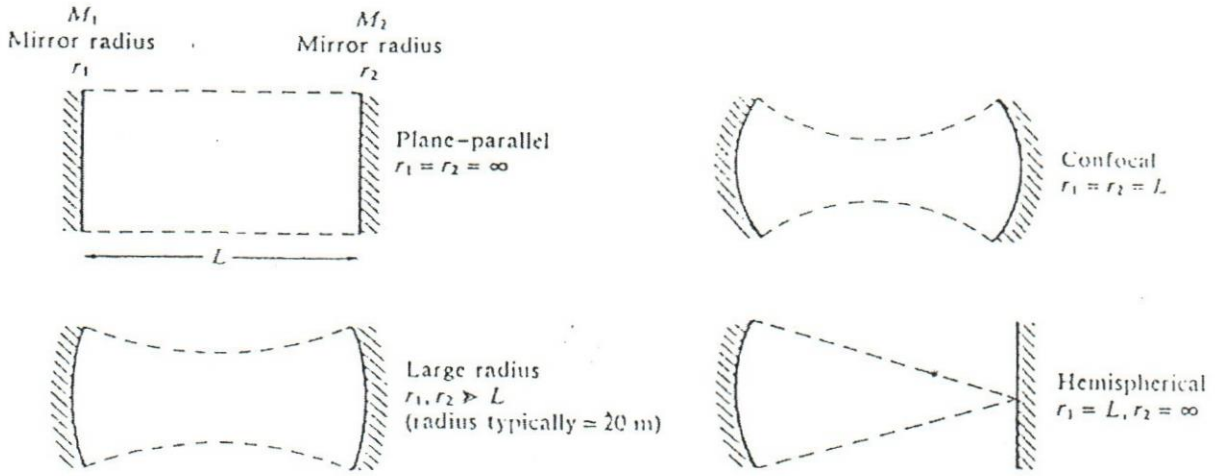

Stable

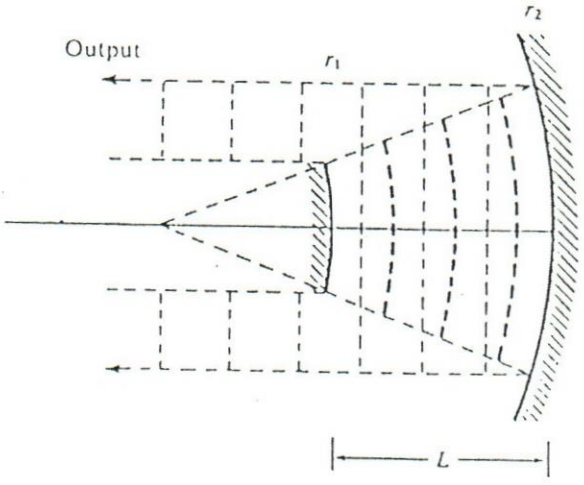

Unstable

Fig 2- 15: Example of stable and unstable resonators greater than the radiation wavelength (After Gold's Borough, 1972).

The plane- concave configuration is frequently used in the CO_2 laser where one of the mirrors can be partially transmitting while the second acts as a planar reflective element for example grating to enable frequency selection. (Seigman, 1986) reported that unstable resonators can be used effectively with high- gain media such as high power CO_2 lasers because these resonators:

1- Eliminate particle reflections.

2- Extract the stored energy from the bulk of laser medium.

3- Allow single mode oscillation at high Fresnel number ($N_F = a^2/ \lambda L$), where a and L are the radius and the length of laser cavity respectively.

2-9 Electrodes

For successful laser operation electrode materials should satisfy certain properties. Electrode materials should be inert to gaseous components involved in the gas mixture. Other properties (Hochuli and Sciacca, 1974) such as very low sputtering rate, having a minimum of negative ions in the sputtered products and consuming no oxygen, are of great importance for a problem- free laser. The most serious problem created by laser electrodes is puttering of the cathode material (Smith, Shield and Webb, 1983; and Hochli et al, 1974). If gaseous compositions of the cathode material are formed, they will travel down the tube colliding with and condensing upon the laser tube walls and optical components. Condensation usually results

in power degradation (Smith et al, 1983). From the experience of (Smith and Browne, 1974), cathodes act as an active catalyst to the reaction: -

$CO_2 \leftrightarrow CO + O$

The results were obtained in a sealed CO_2 laser using CO_2, He, N_2 and Xe mixtures unless other wise specified.

1- Gold: gold sputters very badly with life times surprisingly short in comparison with other materials about the uses of Gold was very few for electrodes.

2- Copper cathodes: it is a good cathodes perform very well in He-CO_2-CO-Xe mixtures. A moving spot was formed at high current densities. Surprisingly, copper performs well only with the exclusion of N_2 from the mixture. This fact was noticed by (Smith at al, 1983) and (Hochuli et al, 1974).

3- Platinum and platinum- Rhodium (90-10):

Both metals showed low loss of CO_2 molecules although sputtering was heavy for both materials.

4- Stainless steel: For comparable of platinum CO_2 loss was low. There was no sputtering. A concluded (Smith, et al, 1983) that stainless steel, especially type 304 which contains (Cr 18%, Ni 10%, 0.5-1% Si, 1-2% Mn and the balance Fe) will make the best electrode for CO_2 lasers. The problem of CO_2 loss and deposition of cathode material on the tube walls can be reduced by pumping out the gas near the cathode and

having the gas flow direction from anode to cathode. In the conventional laser described in this thesis nickel electrodes are used.

Chapter 3

The photoacoustic effect

3-1 Introduction

Photoacoustic (PA) effect was discovered by Bell in 1880. The photoacoustic technique found interest and applications only after the discovery of lasers as first demonstrated by (Kerr and Atwood, 1968). Many researches have shown the versatility of photoacoustic for studies of a wide range of phenomena. The method has as a consequence found an important application in air pollution studies (Dewey,Kam and Hackett 1973, Rosengren, Max and Eng 1974, Goldan and Goto 1974). Rosencwaig, 1980 reported application of the method in physics, chemistry, biology, microelectronics and medicine. The photoacoustic effect is generated by the transfer of photon energy to sound energy and detected by a microphone when an intensity modulated light enters photoacoustic cell filled with the gaseous sample as shown in Fig (3-1), the molecules of the gas absorb all or a portion of incident radiation and are excited into higher rotational- vibrational levels. The collision processes transfer this vibrational energy into transnational energy. In a closed volume this yield a certain gas pressure. Sound is produced if the gas is exposed to a rapidly interrupted incident radiation, which is converted into

an electrical signal by means of a microphone. The steps of the generation to photoacoustic signal is shown in Fig (3-2)

3-2 The photoacoustic theory.

3-2-1 light absorption

The gas molecules are excited from the ground state, E_1 to an excited state, E_2 when they absorb photons having the energy difference between the ground state and the excited state given as:

$E_2-E_1 = h\nu$.....3-1

The excited molecules can then return to ground state by losing their energy in one of the following ways (Rosencawing, 1980): -

1- Radiate dexcitation.

2- By initiating a photochemical event such as bond rearrangement (photochemistry).

3- By colliding with the molecules of other molecules or same species that are in the ground state, $E_1$and excite them to their excited state, E_2.

4- By colliding with any other molecule in the gas and transfer energy to transnational or kinetic energy shared by both molecules i.e. heating. The parameter r_{ij} represent the radiative transition (collisionally) induced transition from E_i to E_j respectively.

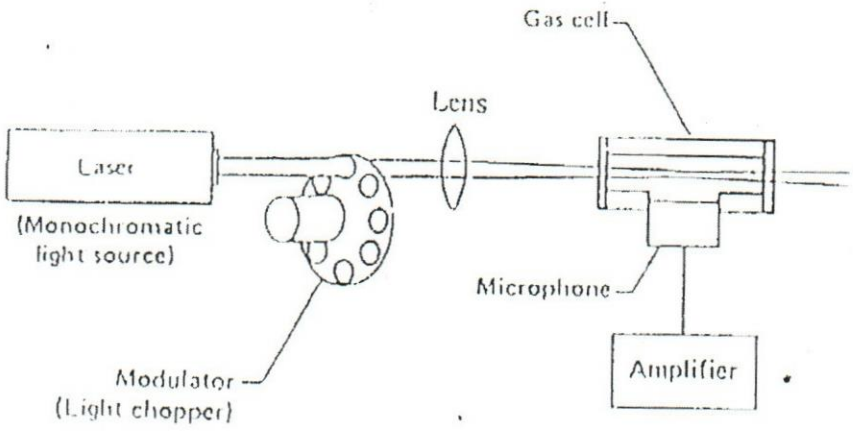

Figure 3-1 Block diagram of a gas photoacoustic spectrometer (After Kreuzer, 1977)

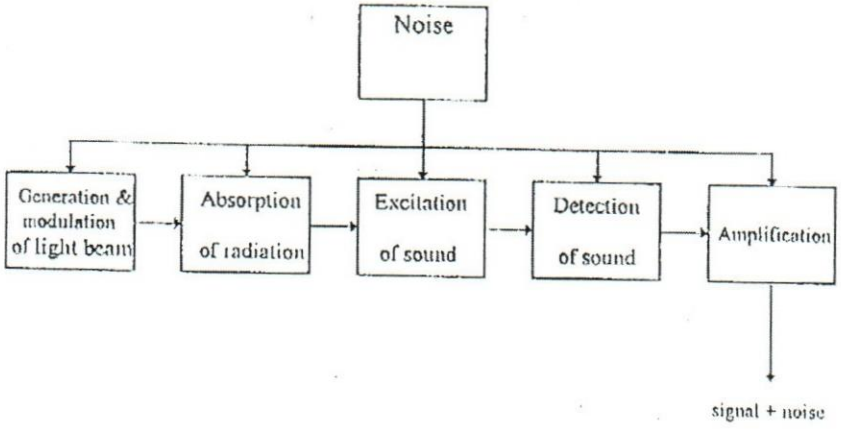

Figure 3-2 The steps in the generation of photoacoustic signal (After Kreuzer, 1977).

$r_{ij} = \rho_v B_{ij} + A_{ij}$ .....(3-2)

Where ρ_v is the radiation density at energy E_v, and E_v, is the energy difference between the energy of the excited state E_2 and the energy of the ground state E_1 ($E_v = h\nu = E_2 - E_1$).

where B_{ji} represent the Einstein coefficient for stimulated emission i to j, and absorption j to i, respectively. A_{ij} represent the Einstein coefficient for spontaneous emission i to j.

3-2-2 Excitation of sound signal.

A significant number of molecules are excited from their ground state E_1 to an excited state E_2 occurs when the incident radiation interacts with the molecules. These excited molecules that decay to the ground state, and the energy difference between these two levels $E_v = E_2 - E_1$ goes into transenational energy. The kinetic energy of the molecules increases, and so the velocities of the colliding molecules. If the rotational and vibrational energies of the molecules are ignored, the total internal energy of the gas per unit volume is given by (Rosencwaig, 1980):

$U = \sum (N_i E_i) + K$ .....(3-3)

Where the summation for all the energy levels i, K is the kinetic energy per unit volume. Since there are only two levels of which one is in the ground state then:

$U = N_2 E_2 + K$.....(3-4)

Where N_2 is the number of molecules in the excited state.

By differentiating equation (3- 4) with respect to time then:

$$\frac{dU}{dt} = \frac{dN_2}{dt} E_2 + \frac{dK}{dt} \quad \text{.....(3 – 5)}$$

Where dU/dt represent difference between the absorbed energy and the radiated energy.

From the laws of thermodynamics:

$$dK = \left(\frac{\delta K}{\delta T}\right)_V dT + \left(\frac{\delta K}{\delta V}\right)_T dV \quad \text{.....(3 – 6)}$$

Where T is the absolute temperature and V is the volume. If the volume is constant, $(\partial K/ \partial V)_T = 0$; then:

$$dK = \left(\frac{\partial K}{\partial T}\right)_V dT = C_V dT \quad \text{.....(3 – 7)}$$

Here C_V is the specific heat per unit volume at a constant volume. By integration of the differential equation (3-7)

$$K = C_V T + f(V) \quad \text{..... (3-8)}$$

Where f(V) is a function dependent on volume but not on temperature. For an ideal gas (P = NkT), where p is the pressure, N is the total number of molecules per unit volume, k is Boltzman's constant. Thus

$$P = \frac{k}{C_V} N[K - f(V)] \quad \text{.....(3 – 9)}$$

By taking the derivative of equation (3-8), $\partial P/\partial t$ is the pressure wave given by:

$$\frac{\partial P}{\partial t} = \frac{k}{C_V} N \frac{dK}{dt} = \frac{k}{C_V}(C_{10} N_1 E_1) \quad \text{.....(3-10)}$$

The photoacoustic-generated pressure measured by the microphone is given by:

$$q = -p \quad \text{.....(3-11)}$$

Where p is the photoacoustic pressure and q is the microphone signal.

There are two cases for limiting intensity. For the first and most usual case I_o is small and the optical pumping term:

$2BI_o << \tau^{-1}$, by overreaching too many equations then q is obtained:

$$q \approx \frac{KE_2 N^2}{C_v w}\left(\frac{\tau}{\tau_C}\right)^2 \frac{2BI_0\delta}{\left(1+w^2\tau^2\right)^{\frac{1}{2}}} e^{i\left(wt-\gamma-\frac{\pi}{2}\right)} \quad \text{.....(3-12)}$$

Where: w is the modulation frequency, τ is the total de-excitation lifetime, τc is the collisional lifetime. Cv is specific heat, I_0 is light intensity. B is equal constant, γ is the specific heat capacity ratio at constant pressure, δ is a factor arising from the modulated intensity at frequency w.

The second case is when $2BI_0 \gg \tau^{-1}$, which represents a high intensity for the optical power per unit area. The photoacoustic signal then becomes for a small value of w:

$$q = \frac{KE_2N^2}{C_v w}\tau_c^{-2}\frac{I}{BI_0}\delta e^{i\left(wt-\gamma-\frac{\pi}{2}\right)} \quad \text{.....(3-13)}$$

Where I is the beam intensity, here absorption saturation occurs where the signal varies, as I_0. This saturation is simply the result by de-excited ($BI_0 > \frac{1}{2}\tau^{-1}$). Experimental evidence of the effect of absorption saturation on the photoacoustic signal has been obtained by Palo and Clasps in 1975.

3-2-3 Photoacoustic detection.

For photoacoustic detection microphones are the most important part of the experiments. Sound signal detection is achieved when the photoacoustic wave creates capacitance change of the microphone, which is transformed, into voltage signal (Vs). The signal is proportional to the biasing voltage and microphone diagram area. The average position of the microphone diaphragm can be written as $X = \frac{1}{2} X(0)$, where X (0) is the full displacement of the diaphragm center. The force exerted on the diaphragm is of two kinds: one resulting from the sound pressure and second kind is result of biasing the microphone, which causes displacement by an amount given by (Kreuzer, 1977):

$$X_0 = \frac{C_m V_B^2}{d K_m} \quad \text{.....(3-14)}$$

Where $K_m = 8\pi T_m$ is called the microphone restoring force, d is the displacement between the microphone plates, C_m is the unbiased microphone capacitance, V_B is the biasing voltage and T_m is the microphone diaphragm stiffness and should be sufficient to stop the bias voltage from bringing the diaphragm into contact with the back plate of the microphone. The microphone is connected to a bias voltage through a ballast resistor in one of two possible ways: (1) the electric charge on the diaphragm is kept constant and the signal is detected as voltage using high impedance amplifier. (2) The voltage remains constant and the signal is detected as a current using a low impedance amplifier.

3-3 Photoacoustic resonators.

Photoacoustic resonators are cavities in which photoacoustic signal is being generated. Resonators can take many shapes and forms, but can be categorized into two main types. In the following a brief description of both types will be discussed.

3-3-1 Helmholtz resonators

The resonator consists of a bottle almost entirely enclosing a volume of air, with a small opening, or neck, constituting a coupling between the air

in the bottle and the external air of the room. The dimension of the resonator are small compared with a wavelength of sound (William, 1955).

It is essentially a rigid container, with an opening to the surrounding air. Fig (3-3) shows the cross section of two different types of Helmholtz resonators. The resonator in Fig (3-3 a) has a simple circular opening, while that in Figure 3-3b has a short attached cylindrical neck. If a tuning fork of a frequency to which the cavity resonates is held near the opening, the sound intensity in the neighborhood will be greatly enhanced. As a result of the following analysis, it is possible to predict with fair accuracy the natural frequency of the resonator, subject to important restrictions placed upon the dimension of the resonator (Robert, 1951). The resonator with the attached neck is simpler to analyze and what follows will apply to this type. As shown in Figure 3-3b, V_o represents the volume of the main cavity, while S and ℓ are the cross sectional area and length of the neck respectively. All dimensions are assumed small compared with wavelength of sound in air λ. If a source of energy such as vibrating tuning fork is held near the opening. Some of the energy radiated towards the resonator will set into vibration a cylindrical plug of air within the neck of volume ℓS. This plug of air may be assumed to move as a unit (since $\ell << \lambda$) under the action of the driving force to the tuning fork, the elastics force on the inner end of the plug (due to compressibility of air enclosed in the volume V_o)

and force of dissipation. This last force is due mainly to the radiation of sound energy and may be expressed in terms of acoustic radiation impedance, as we shall soon see.

The equation for the motion of the air in the neck, treating the air plug as particle is given by:

(Masses) (Acceleration) = $F_{driving} + F_{dissipative} + F_{elastic}$.....(3-15).

In this equation, The mass is that of the air plugs, $\rho_o \ell S$, whereρ_o is the average undisturbed density of the air. To evaluate the dissipate term, by using of the acoustic impedance. Neglecting friction in the neck, the main force of dissipation that is associated with the radiated sound energy and there fore with the real part of the acoustic impedance at the right hand end of the plug of air. As the plug oscillates, its right hand face acts as a single source, giving rise to sound waves. The generating surface may be considered a circular plane area. However, the diameter of this circle, like the other dimension of the resonator, is small compared with λ. A surface of any shape whose dimensions are much less than λ will give rise to a wave shape which is spherical at a distance not far from the source, due to diffraction effects. In general the force attached at any section is equal to pressure cross-sectional area.

The force dissipation is given by:

$F = -P_{dis}S = -\rho_o ck^2/2\pi(S^2\varsigma)$,.....(3-16)

Where ς is the velocity of the air next to the surface of the plug, or that of the plug itself.

The elastic force is a result of the spring like effect of the air enclosed in the cavity upon the left-hand end of the plug of air. It is important to note that the diameter of the cavity is small compared with λ.

The magnitude of the elastic force on the air in the neck given as:

$$F = SP_{elastic} = -S\rho_o c^2(\upsilon/V_o) \quad \text{.....(3-17)}$$

Where υ equal to $S\varsigma$ represent the motion of the plug of air (Robert, 1951). If a resonator of volume V_o fitted with a short neck of effective length ℓ, and sectional area S. The air in the neck as shown in figure 3-3-b is assumed to act as a plug p, which moves and frowned the influence of external stimulus and the resulting pressure variation within the volume of the resonator (Stephens, 1955).

In the displaced position of the plug as seen in figure 3-3-b, the volume of air to the plug is $V_o+S\ell$ and the pressure is changing for δP to $P-\delta P$, the original value being P, where the quantity δP is the pressure difference acting on the plug and so the actual restoring force equal to m (-a), where m is the effective mass of the plug of air, and a is the acceleration, and hence

$$\delta P = -\ell\rho_o a \quad \text{..... (3-18)}$$

It found that resonance frequency for different volume of a Helmholtz cell by equation given as:

$$W_H = C_0\left(\frac{A}{L_C Vr}\right)^{1/2} \quad \text{.....(3-19)}$$

Where C_0 is the speed of sound in the mixture gas, A is the cross section area of cell, L_C is the length of cell, and V_r is the resonance volume that can be given as:

$$V_r = \frac{V_{cavity} \times V_{cell}}{V_{cavity} + V_{cell}} \quad \text{.....(3-20)}$$

Where V_{cavity} is the volume of the laser cavity, and V_{cell} is the volume of the Helmholtz cells.

Finally resonance frequency about the last equations is given by:

$f_{res} = W_H/2\pi$.....(3-21)

The last equation is used to calculate the Helmholtz resonance frequency for a cell with neck. On the other hand if the Helmholtz cell is neckless then the resonance frequency is given by the relation: -

$$f_{res} = \frac{C_0}{2\pi}\sqrt{\frac{2r}{V}} \quad \text{.....(3-22)}$$

where r is the radius of pipe and, C_o is the speed of sound in the mixture gas. From equation (3-22) it is concluded that:

$$f_{res}^{\ 2} \propto \frac{1}{V} \quad \text{.....(3 – 23}$$

i.e $(f_{res})^2$ V = constant for a particular Helmholtz cell.

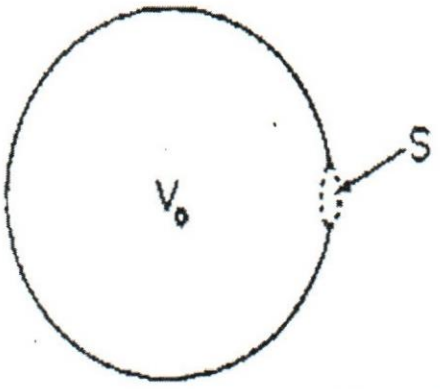

Helmholtz resonator without "neck"

(a)

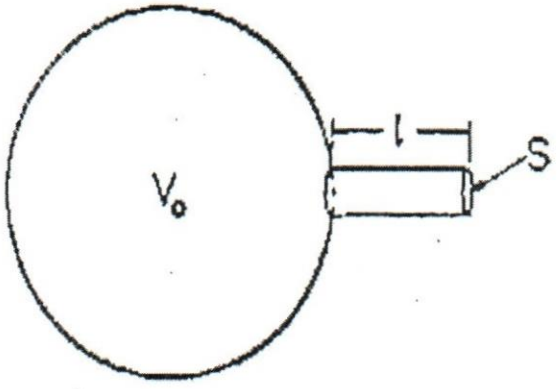

Helmholtz resonator with "neck"

Figure 3-3 Types of Helmholtz resonators, (a) Helmholtz resonator with out neck, (b) Helmholtz resonator with neck (After Robert, 1951).

3-3-2 Other types of (PA) cells

The PA cell is aimed towards the maximum possible signal to noise ratio. Cells have been constructed of different sizes and shapes (Rosencwaig, 1980). Bruce, Sojika, Hurd, Watkins, White and Derzko (1976) as shown in figure 3-4a used the first cell for acoustic detection. Another type that involves an open photoacoustic cell placed in a larger container has been employed by Shtrikman and Slatkin (1977). The background signal was reduced to signal equal 20 parts per billion of ethylene in N_2. A similar idea has been used by Lehmann et al, (1982) where a waveguide 2.2mm x 5mm x 18cm long was used in a larger container as shown in figure 3-4b. Another type of cell is described as a cell body made up of 180-mm-long tube (pipe) of new silver alloy (I.d.9mm wall thickness 0.5mm) closed both ends by ZnSe Brewster windows (Henk and Bicaric, 1989). This type of cell used in pulsed photoacoustic spectroscopy. It must be of different design from those used in Cw PAS, in order to minimize extraneous signals generated by the large photon fluxes provide by pulsed laser sources. These types suggest a sample cell such as that shown in fig 3-4-c. The windows must be scrupulously cleaned and should be of the highest possible optical quality to minimize absorption at scattering from the cell windows, (Virupaksha, 1983).

The proper choice of the PA cell geometry depends on the intended application. For gas- phase measurements, mainly resonant cells are combined with appropriately chopped cw lasers. On the other hand, investigations of molecules absorbed on surfaces, of this surface layers, or of phase transitions (e.g., for liquid crystals) are performed by use of acoustic or piezo electrical response to a laser pulse, thus avoiding sophisticated acoustically resonant cells, (Zharov, 1986).

The PA signal decreases with higher modulation frequencies, therefor

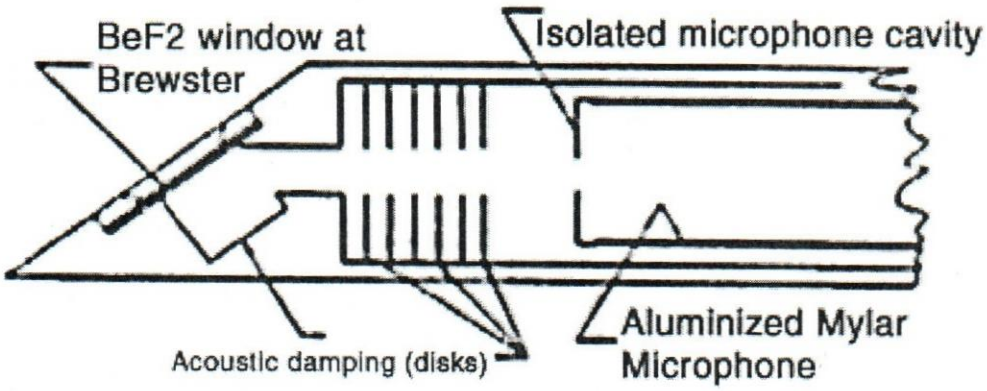

Figure 3-4a Schematic of a photoacoustic cells that employs acoustic baffles. (After Bruce et al, 1976)

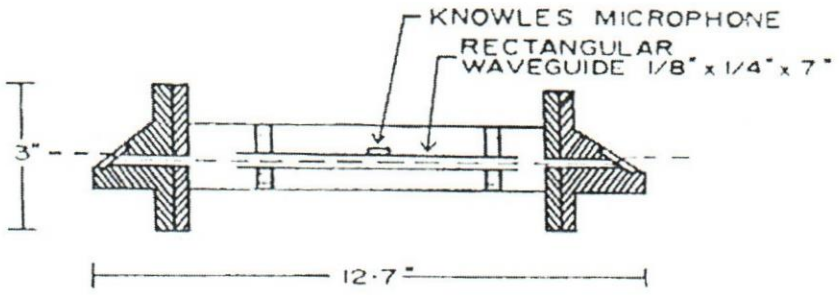

Figure 3-4b: A resonant photoacoustic cell placed in larger container to reduce window heating. (After Lehmann et al, 1982).

It is advantageous to use low modulation frequencies. To decrease the microphone response to window absorption, one has to increase the length of the cell, since the energy absorbed by the windows is then distributed over a large volume.

For a resonant cell, one has to multiply the above cell constant F with the quality factor Q of the generated acoustic resonance:

$$f_{res} = \frac{G(\gamma - 1)\ell_r Q}{WV_r} \qquad (3-24)$$

Where G is geometrical factor, $W=2\pi f$ is the modulation frequency, γ is the specific heat constant, ℓ_r and V_r is the length and the volume of the acoustic resonator respectively, and Q equals the ratio of the energy stored in the acoustical standing wave over the energy losses per cycle.

At resonance, external acoustical noises within the cell will a pear amplified for a high Q value of a resonant cell. Here acoustical shielding helps, i.e., proper cell-wall construction, material choice, and good design of inlet and outlet ports are required as shown in figure 3-4-d. In the previous figure two PA cells are distinguished:

(a)The Zurich banana cell, the laser beam enters from the left through a Brewster window to leave the central part ($\ell = \lambda/2$) of the resonator at the right Brewster window (BW). The position of the microphone M is indicated. The two pieces before and after the bents of length of ($\lambda/4$) serve to suppress the window signal. The total lengths of the banana cell a mount to λ. In the bents the gas inlet and gas outlet (Gi and Go) are shown.

(b) The Harvard-Nijmegen open-organ-pipe cell, the main part is manufactured of a block of massive aluminum. The central organ

Pipe acts as an open resonator with length ($\lambda/2$), the copper tube has a highly polished, gold-coated inner surface to minimize wall heating by stray light. The central gas inlet (Gi) is essential to obtain short measuring times, only the resonator volume of 2.8 mL must be replenished before an independent concentration measurement can be performed. TAC: $\lambda/4$ tunable air columns to suppress window signal. NF: $\lambda/4$-notch filter to suppress acoustic in coupling of noise via gas inlet. The idea about this type of cells is to fill both cells with non-absorbing gas. In this case the

background signal will be measured. When designing a PA cell at high temperature, two possibilities must be followed. First, the microphone and the cell must be the same temperature. Second, the microphone is maintained at room temperature while the remaining sections of the cell are being heated, (Henk and Bicaric, 1989). The heat pipe is advice that effectively transfers heat by perpetually boiling and condensing the fluid under investigation. The versatility of PA heat pipe (PAHP) has been demonstrated by recording the absorption spectrum of geraniol $C_{10}H_{18}O$ at CO_2 laser wavelength.

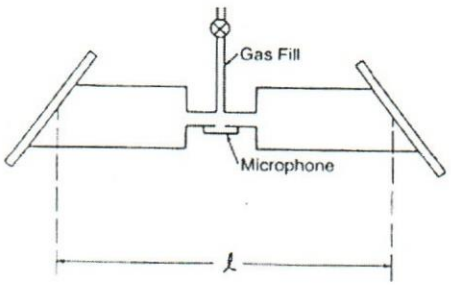

Figure 3-4-c Sketch of a cell appropriate for use in pulsed photoacoustic experiment (After Virupaksha, 1983).

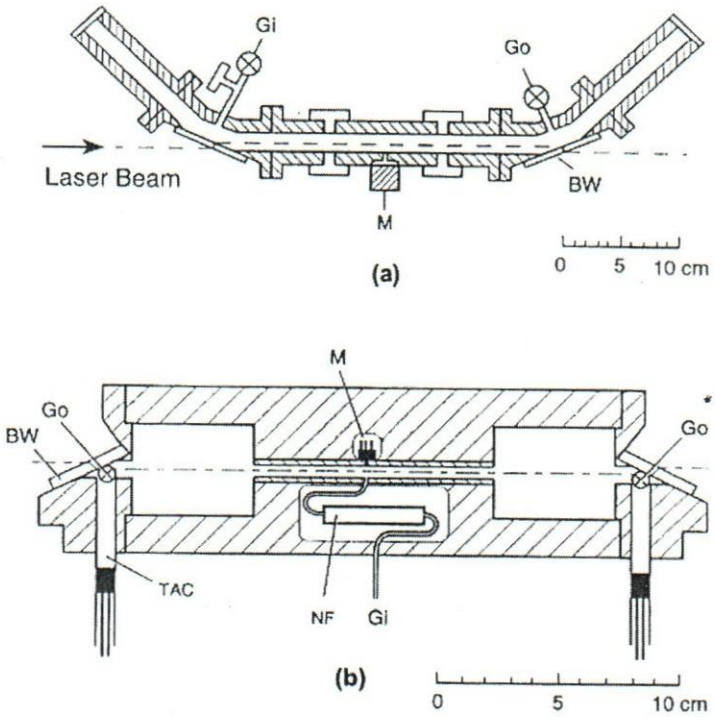

Figure 3-4-d Two PA- cell types successfully used in trace-gas detection (After Harren and Reuss, 1997).

The PAHP cell described in fig 3-4-e consists of five major parts

(a) The cylindrical body heater H, (b) water cooling H_2O,

(b) Microphone M, (d) wick Wi, (e) Brewster windows W.

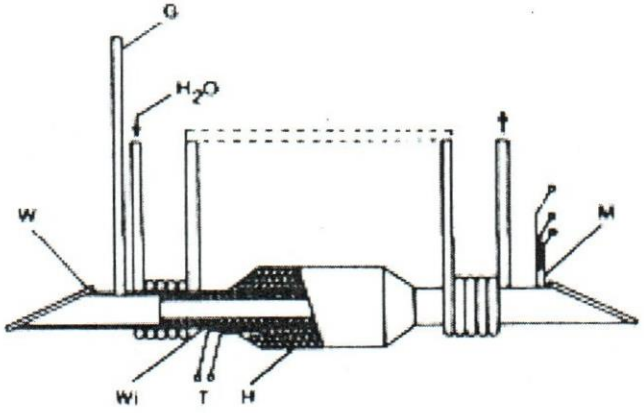

Figure 3-4-e Design of the PAHP, heater element (H), thermocouple (T), microphone (M), Brewster window (W), wick (Wi), gas inlet (G), and water cooling (H_2O), (After Henk and Bicanic, 1989).

To find the resonance frequency at radial, and or longitudinal modes the following equation can be used:

$$f_{res} = \frac{C_0}{2}\left[\left(\frac{nz}{L}\right)^2 + \left(\frac{\alpha mm}{a}\right)^2\right]^{1/2} \quad \text{.....(3-25)}$$

Where C_0 is the sound speed of the sample, f_{res} is the resonance frequency, nz, n, m are the eigen value related to longitudinal, azimuthal and radial modes respectively, αmm is the nth root of the equation involving the mth order Bessel function, a is the radius of the cell and L is the length of the cell. The resonance frequency for the lowest radial mode is found for $(nz = 1,\ n = m = 0)$.

Chapter 4

Laser cavity photoacoustic data

4-1 Introduction

The results to be discussed here are derived from previous work performed by two researchers Abu-Taha, 1987 and later by Parslow, 1993 for conventional and waveguide lasers respectively. Although Abu-Taha has suggested and used the Helmholtz resonator to detect the (PA) signals in a waveguide cavity, his results were concentrated on the conventional laser cavity. The duty of this thesis is to compare the results from both works for the two types of lasers to give more insights of any differences or agreements and its importance in understanding what is happening in the laser cavities. In the following a brief description of the detection schemes from both works will be given and will be followed by tables of measured resonance frequencies at the different conditions. Graphs will be viewed here and discussed in the next chapter.

4-2 Intracavity signal detection

The intracavity (PA) signal detection can be a cheived simply by attaching a microphone to laser cavity wall. Anyhow special fitting can be designed to allow suitable inclusion of the detection unit without interruption to the laser cavity and at the same time keep the microphone at a safe location from the voltages and temperatures of the discharge region.

The cavity in this case acts as a complicated PA cell, in a sense that it contains a discharge region that is different from other regions outside it, where gas temperature and properties are different. Laser cavity is also connected to gas in and out tubes, which adds up to the cavity volume i.e. PA signals can be detected in these tubes as well. One way to avoid microphone damage is to allow gas in the region between a microphone and discharge region. Also care must be taken that the microphone is far enough from the nearest electrode, since arcing to the microphone can easily kill it.

4-3 Photoacoustic signal detection in the conventional laser cavity

Photoacoustic signal was detected for the first time (Abu-Taha, 1987, Abu-Taha and Laine, 1989). A stainless steel tube 2cm internal diameter as shown in figure 4-1 and 6cm long was fitted with a microphone in the middle was connected to the laser tube from the anode end at one side to the mirror holder from the other (see figure 4-2). Other materials were used to manufacture the cell with almost the same results. The input signal from the microphone was fed into a phase sensitive detector. Modulation was acheived using a piezo tube attached to the grating. Also chopping was possible by placing a mechanical chopper in the gap between the Brewster window and the grating.

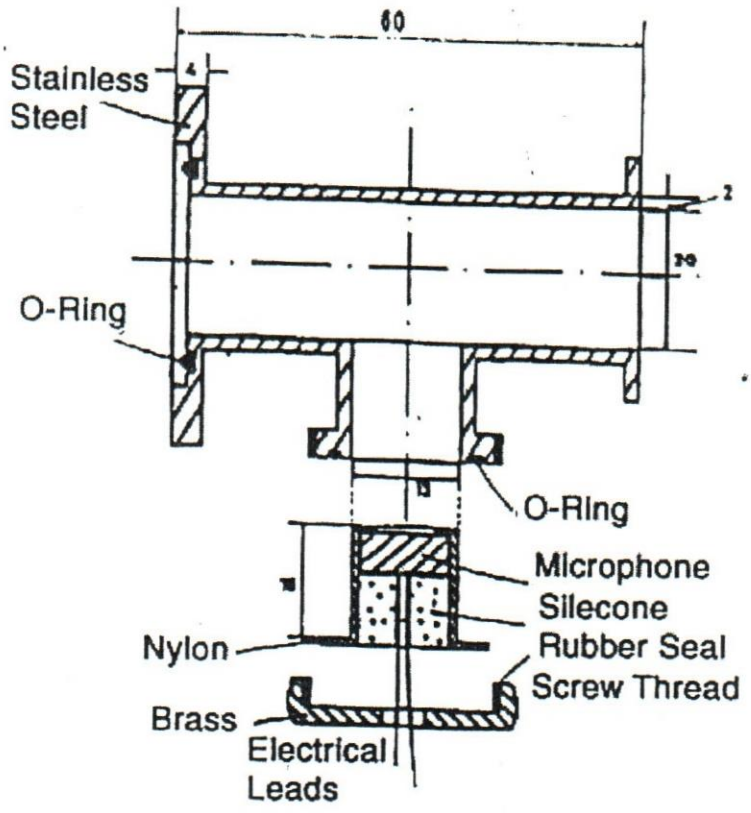

Figure 4-1 Intracavity cell (self-absorption) for PA detection in conventional CO_2 laser (After Abu-Taha, 1987).

The total length of laser cavity from mirror to the Brewster window is nearly 190cm. It should be kept in mind that the laser cavity has a uniform diameter nearly 1cm, in most of length nearly 150cm, where the rest of the length has a larger length nearly 2cm. The microphone is the most common sensor for PA detection. An electrical signal across the microphone is created when the PA wave creates a capacitance

charge of the microphone, which is then transformed, into voltage signal.

4-4 Photoacoustic signal detection in the waveguide laser cavity

The main application of the photoacoustic signal detected in the laser cavity is to be used in the stabilization of the CO_2 waveguide laser. The signals are obtained in a differential form, resulting from the frequency modulation of the laser cavity. It used a microphone to observe the pressure variation arising from the absorption of the modulated laser radiation in the wg cavity.

This microphone has a flat frequency response between 0.1 and 2KHz and exhibits a low sensitivity to vibration. Since the microphone is a delicate device it must be shielded from the discharge, and any earthing of the discharge. The modulation of the wg laser was also achieved by placing a piezo- electric element on the diffraction grating. The grating rested upon two pieces of o- ring material giving a spring effect for the piezo. The microphone signal was detected using a lock-in amplifier, Stanford Research System SR- 150. Remote microphone on the end of an18cm Teflon tubes, with an internal diameter of 2mm, leading from the Brewster window. Later three microphones constitutes the first trail was used and distributed in different pourboires as shown in figure 4-3.

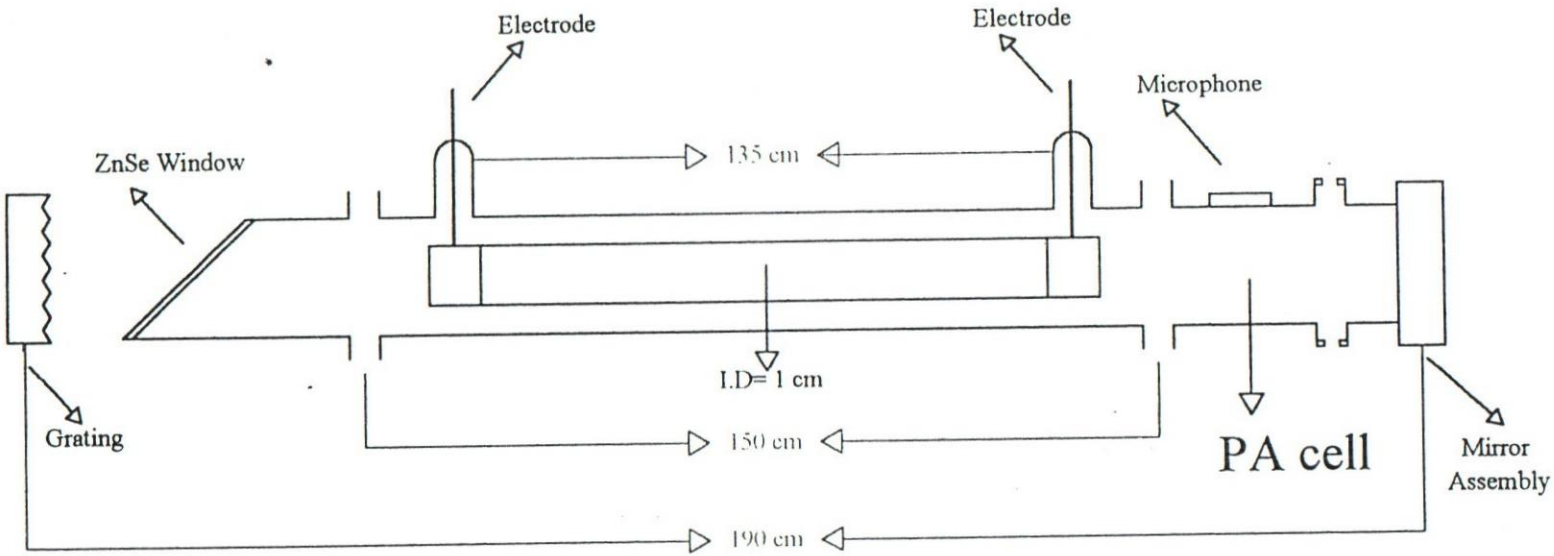

Figure 4-2 Schematic of the conventional laser system for PA signal detection by (Abu - Taha, 1987).

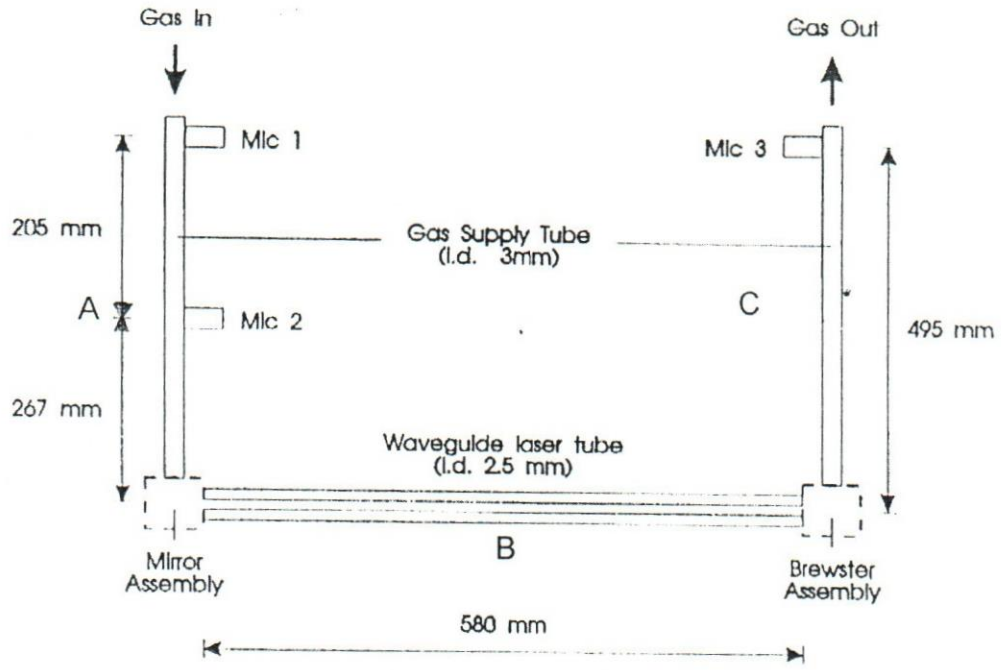

Figure 4-3 Positions of microphones used by (Parslow, 1993) to detect intracavity PA signals in the CO_2 waveguide laser cavity.

A rotary chopper placed between the laser and amplifier to modulate the laser beam at any frequency that may be required. The speed of sound in a gas at different temperature is calculated by multiplying the values given in table 4-1 by temperature dependent factor:

$$\sqrt{\frac{T}{273.16}} \quad \text{.....(4-1)}$$

where T is the temperature of the gas in Kelvin and the speed of sound in a mixture of gases as reported by (Parslow, 1993):

$$C_o = \left[\frac{RT}{M}\left(1+\frac{R}{C_V}\right)\right]^{1/2} \quad \text{.....(4-2)}$$

Where R is the gas constant, M the molecular weights of the mixture and C_V the average weighted of the specific heat at constant volume of the mixture.

Constituent gas	**Speed of sound at 0°C (ms^{-1})**
CO_2	280
N_2	354
He	972

Table 4-1: Speed of sound, at 0°C, in the constant gases used in the CO_2 waveguide laser.

The temperature of the gas mixture during laser operation is equal to 400 Kelvin. The calculated speed of sound for laser mixture is equal to 790 m/s.

4-5 Experimental data

The results sited here are PA resonances derived from experimental results performed using a conventional and a waveguide laser. In both cases the microphone was the main sensor used to detect the signal. Results will also be calculated theoretically for the sake of comparison with the experimental results. It is worth mentioning that the resonance frequencies reported in this work are derived from the experimental work of (Abu-Taha, 1987 and Parslow, 1993).

4-5-1 Waveguide laser data

The initial experimental result were taken from a remote microphone on the end of an 18cm Teflon tube, with an internal diameter of 2mm, leading from the Brewster window assembly. Later three microphones are fitted in the positions shown in figure 4-2. The dependence of the signal strength on the level of modulation is shown in table 4-2,4-3,4-4. The results were taken at constant laser gas pressure of 60torr.

4-5-2 Conventional laser data

The results reported here were the first of its kind for PA detection in a laser cavity by (Abu-Taha, 1987). The photoacoustic signals were detected at different frequencies, currents and pressures as seen in table 4-5-16.

Signal ampl./arb.units	Resonance freq.(Hz)
2.10	191
2.90	500
3.80	787
4.20	1125
3.10	1490
1.80	1840
1.10	2280
0.80	2735

Table 4-2: PA signal versus modulation frequency at constant current and a pressure of 60 torr, as detected by microphone (1) in the position shown in figure 4-3 (After Parslow, 1993).

Signal ampl./arb.units	Resonance freq.(Hz)
2.00	250
4.20	670
5.40	1170
4.00	1655
2.20	2340

Table 4-3: PA signal versus modulation frequency at constant current and a pressure of 60 torr, as detected by microphone (2) in the position shown in figure 4-3 (After Parslow, 1993).

Signal ampl./arb.units	Resonance freq.(Hz)
0.75	205
0.92	470
0.96	810
0.70	1170
0.55	1525
0.30	1895
0.15	2395

Table 4-4: PA signal versus modulation frequency at constant current and a pressure of 60 torr, as detected by microphone (3) in the position shown in figures 4-3 (After Parslow, 1993).

Signal ampl./arb.units	Resonance freq.(Hz)
-2.3	325
1.4	805
0.2	1860

Table 4-5: PA signal versus modulation frequency at constant pressure of 14 torr and a current of 12 mA, including negative and positive phase signals (After Abu-Taha, 1987).

Signal ampl./arb.units	Resonance freq.(Hz)
-2.5	360
1.65	942
0.2	2060

Table 4-6: PA signal versus modulation frequency at constant pressure of 16 torr and a current of 12 mA, including negative and positive phase signals (After Abu-Taha, 1987).

Signal ampl./arb.units	Resonance freq.(Hz)
-3	323
1.95	735
0.2	1860

Table 4-7: PA signal versus modulation frequency at constant pressure of 18 torr and a current of 12 mA, including both positive and negative phase signals (After Abu-Taha, 1987).

Signal ampl./arb.units	Resonance freq.(Hz)
-3.5	275
1.9	820
0.2	2030

Table 4-8: PA signal versus modulation frequency at constant pressure of 20 torr and a current of 12 mA, including both positive and negative phase signals (After Abu-Taha, 1987).

Signal ampl./arb.units	Pressure (torr)
-2.0	14
-2.5	16
-2.4	18
-2.7	20

Table 4-9: PA signal versus pressure at constant frequency of 360 Hz and a current of 12 mA, (After Abu-Taha, 1987).

Signal ampl./arb.units	Pressure (torr)
0.25	14
1.40	16
0.20	18
0.60	20

Table 4-10: PA signal versus pressure at constant frequency of 942 Hz and a current of 12 mA, (After Abu-Taha, 1987).

Signal ampl./arb.units	Resonance freq.(Hz)
0.8	234
-1.4	555
0.3	925
0.13	2160

Table 4-11: PA signal versus modulation frequency at constant current of 12 mA, and a pressure of 18 torr, including both positive and negative phase signals (After Abu-Taha, 1987).

Signal ampl./arb.units	Resonance freq.(Hz)
0.75	188
-1.05	620
0.23	1025
0.1	2230

Table 4-12: PA signal versus modulation frequency at constant current of 16 mA, and a pressure of 18 torr, including both positive and negative phase signals (After Abu-Taha, 1987).

Signal ampl./arb.units	Resonance freq.(Hz)
0.4	192
-0.65	600
0.15	958
0.07	2160

Table 4-13: PA signal versus modulation frequency at constant current of 20 mA, and a pressure of 18 torr, including both positive and negative phase signals (After Abu-Taha, 1987).

Signal ampl./arb.units	Resonance freq.(Hz)
0.3	220
-0.55	655
0.1	1025
0.07	2160

Table 4-14: PA signal versus modulation frequency at constant current of 24 mA, and a pressure of 18 torr, including both positive and negative phase signals (After Abu-Taha, 1987).

Signal ampl./arb.units	Current (mA)
-1.35	12
-1.05	16
-0.60	20
-0.50	24

Table 4-15: PA signal versus current at constant frequency of 620 Hz and at a pressure of 18 torr (After Abu-Taha, 1987).

Signal ampl./arb.units	Current (mA)
0.30	12
0.15	16
0.10	20
0.05	24

Table 4-16: PA signal versus current at constant frequency of 925 Hz and at a pressure of18 torr (After Abu-Taha, 1987).

4-5-3 Theoretical versus measured resonances

Every acoustic cavity has a resonance frequency to which it responds. This frequency can be calculated theoretically. Due to the complex nature of the laser cavity i.e. it is not simple from the point of view that the main laser cavity that contains the active medium has many leading gas pipes attached to it. It is known by (Wood, 1955) that for a Helmholtz cells the shapes are not an important factor and the key role is related to the volume of cells. One important condition is that the dimension of the neck should be very much less than the rest of the cell. Theoretically resonance frequencies can be calculated using equations (3-21), (3-22), and (3-25). In the present work many trials using the above equations were carried out to establish an idea of the relation that allow the calculation of the resonance frequencies in the laser cavity and compare the experimental and calculated frequencies. In doing so many problems were encountered, for example the main laser cavity has diameters, but to it attached other tube sections of various diameters. More than that it was extremely difficult to assign the exact volume of the cell and if it can be considered a Helmholtz cell or otherwise.

The above mentioned equations were used in conjunction with certain parts of the laser as cavity, for example in figure 4-3 for microphone (1), the part in A is assumed by itself as neckless cavity. In one trial, (A+B) is the neckless cell and in another (A+B+C). The frequencies calculated

from each trial were compared with the experimentally deduced frequencies from the curves produced by (Abu-Taha, 1987) and (Parslow, 1993). Some coincidences were found although not exact values but very close within the expected practical difficulties. For example for Parslow work and using equation (3-25) there is a close calculated frequency of 836 Hz to that of measured 787 Hz and 2153 Hz as compared with 2280 Hz (see table 4-2). Using equation (3-21) it is found that the signal of the largest amplitude i.e. 1125 Hz is 3 times the theoretical frequency of 360 Hz. This might be considered as one of the harmonic frequencies being excited. If the neckless cavity is assumed for microphone one a frequency calculated to be 2015 Hz the nearest to this is the 2280 Hz. For microphone two also for the largest amplitude frequency 1170 Hz it is 3 times the calculated 360 Hz as found for microphone one. Also near coincidences using equation (3-25) of 1519 Hz and the 1655 Hz. The neckless approximation 2015 Hz is slightly far off the 2340 Hz (see table 4-3). For resonances recorded by microphone three, there is a good approximate calculated frequencies using equation (3-25) of 798 Hz with the signal of the highest amplitude recorded by this microphone namely the 810 Hz, and with the lowest amplitude signal at 2395 Hz compared to the calculated value of 2153 Hz using equation (3-22).

As far as the conventional laser is concerned a very good fit with the calculated frequency using equation (3-25) which gave a theoretical value of 809 Hz compared to the measured value of 805 Hz at a pressure of 14 torr (see table 4-5). More close values of 823, 837 and 850 Hz compared with frequencies detected at the pressures 14, 20 and 16 torr respectively (see tables 4:5, 4.8, 4.6). The relevance of this comparison between the measured and calculated frequencies will be dealt with in chapter 5.

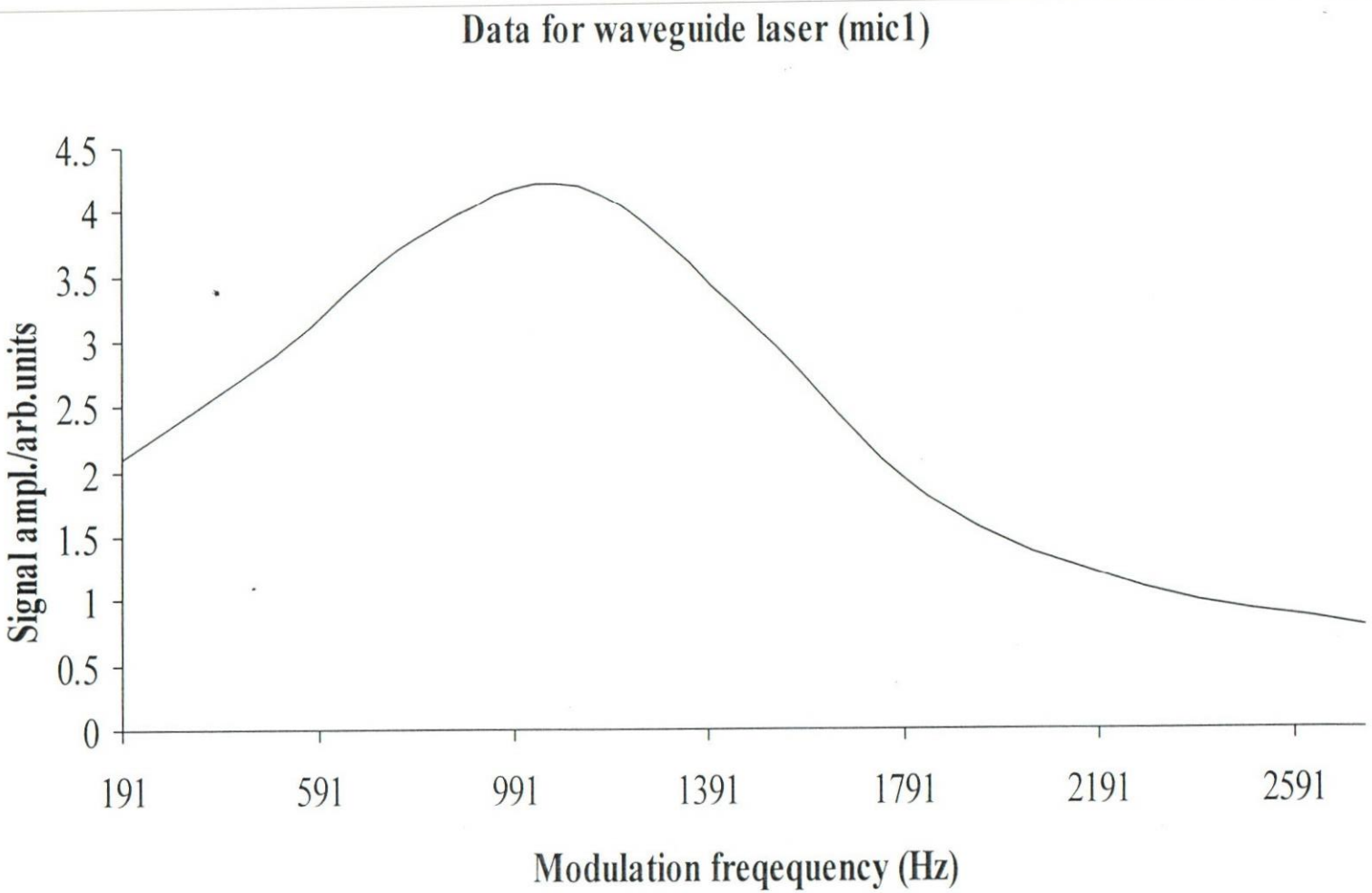

Fig. 4-4: PA signal versus modulation frequency at constant current and a pressure of 60 torr.

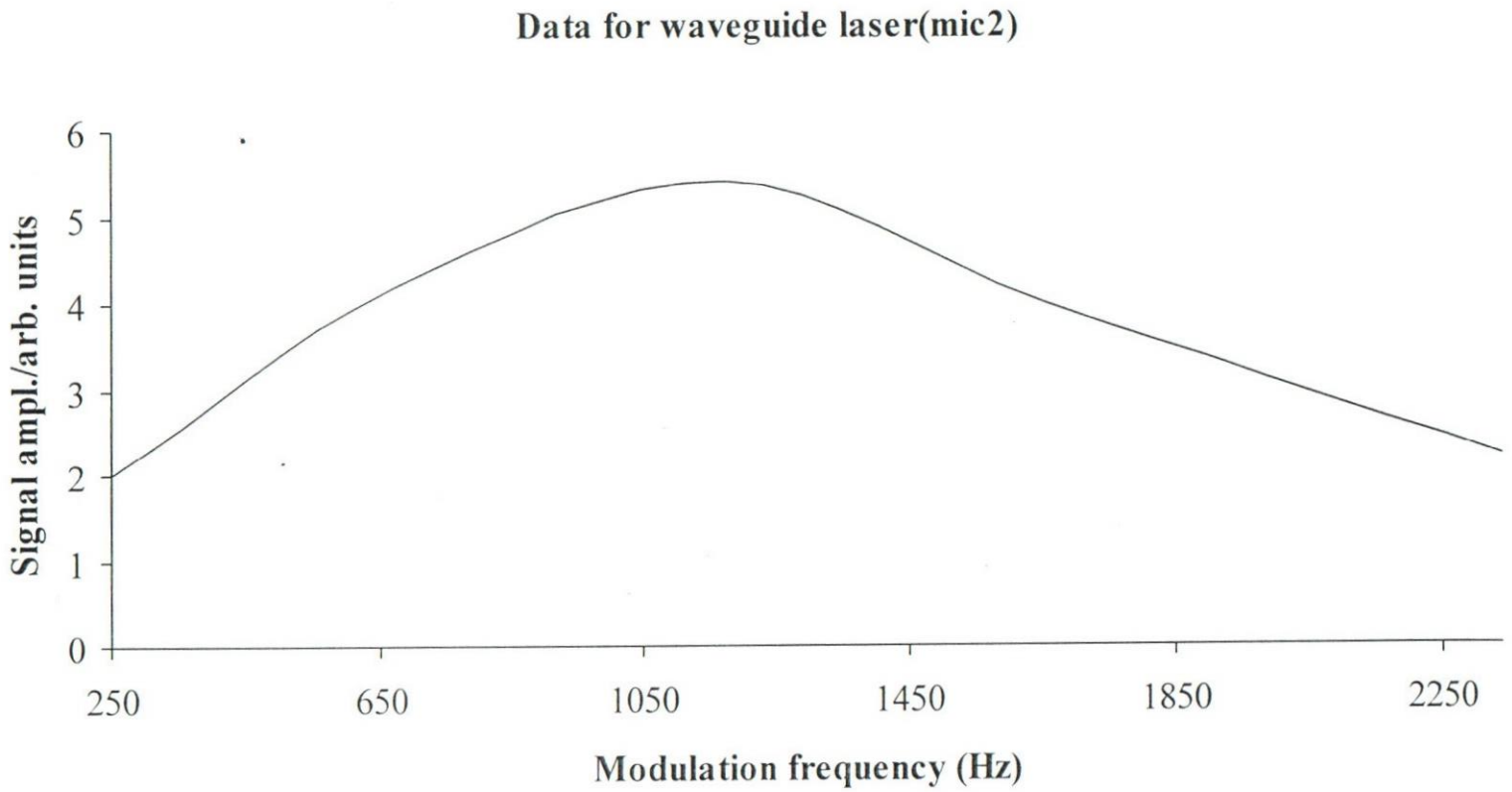

Fig. 4-5: PA signal versus modulation frequency at constant current and a pressure of 60 torr.

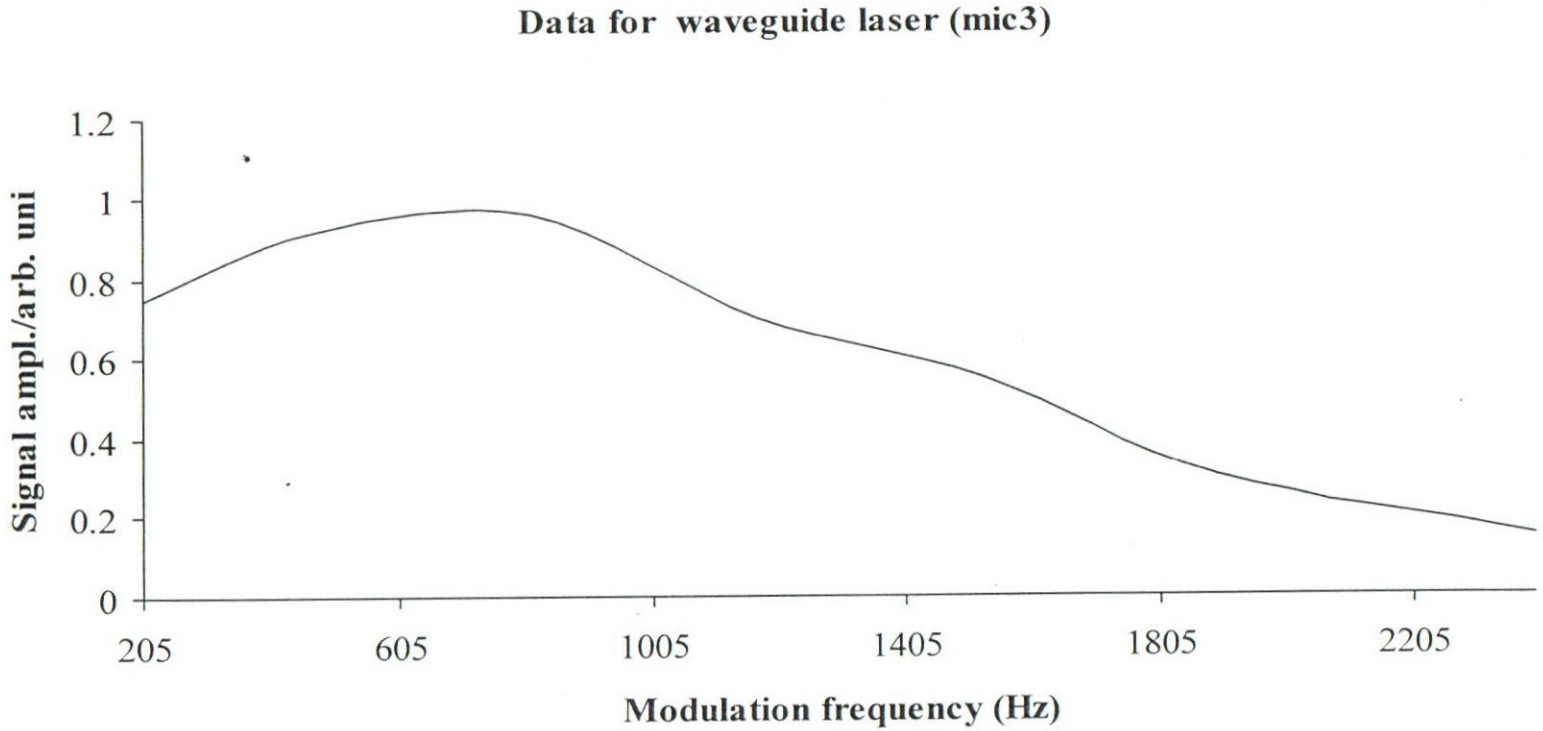

Fig. 4-6: PA signal versus modulation frequency at a pressure of 60 torr and constant current.

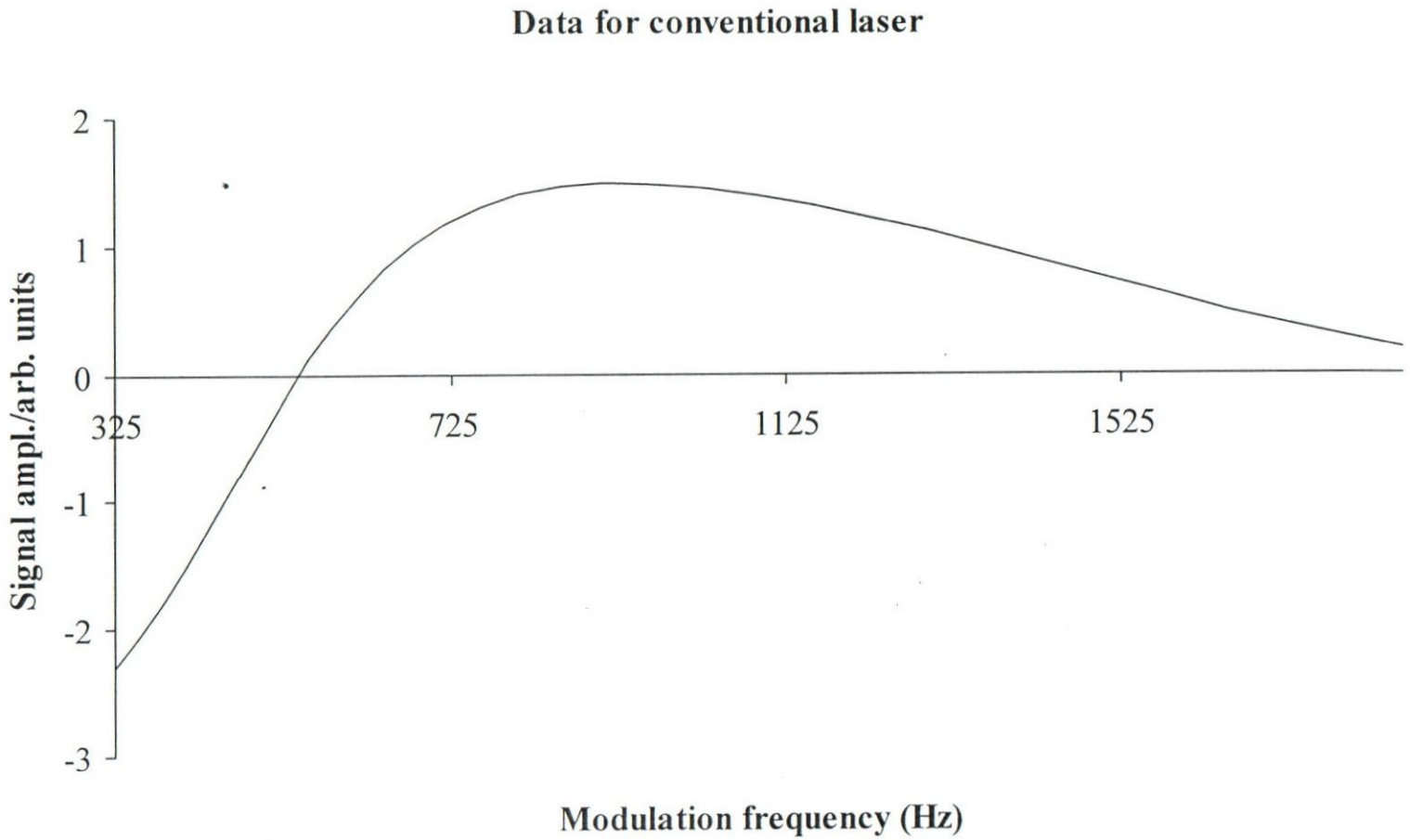

Fig. 4-7: PA signal versus modulation frequency at constant pressure of 14 torr and a current of 12mA.

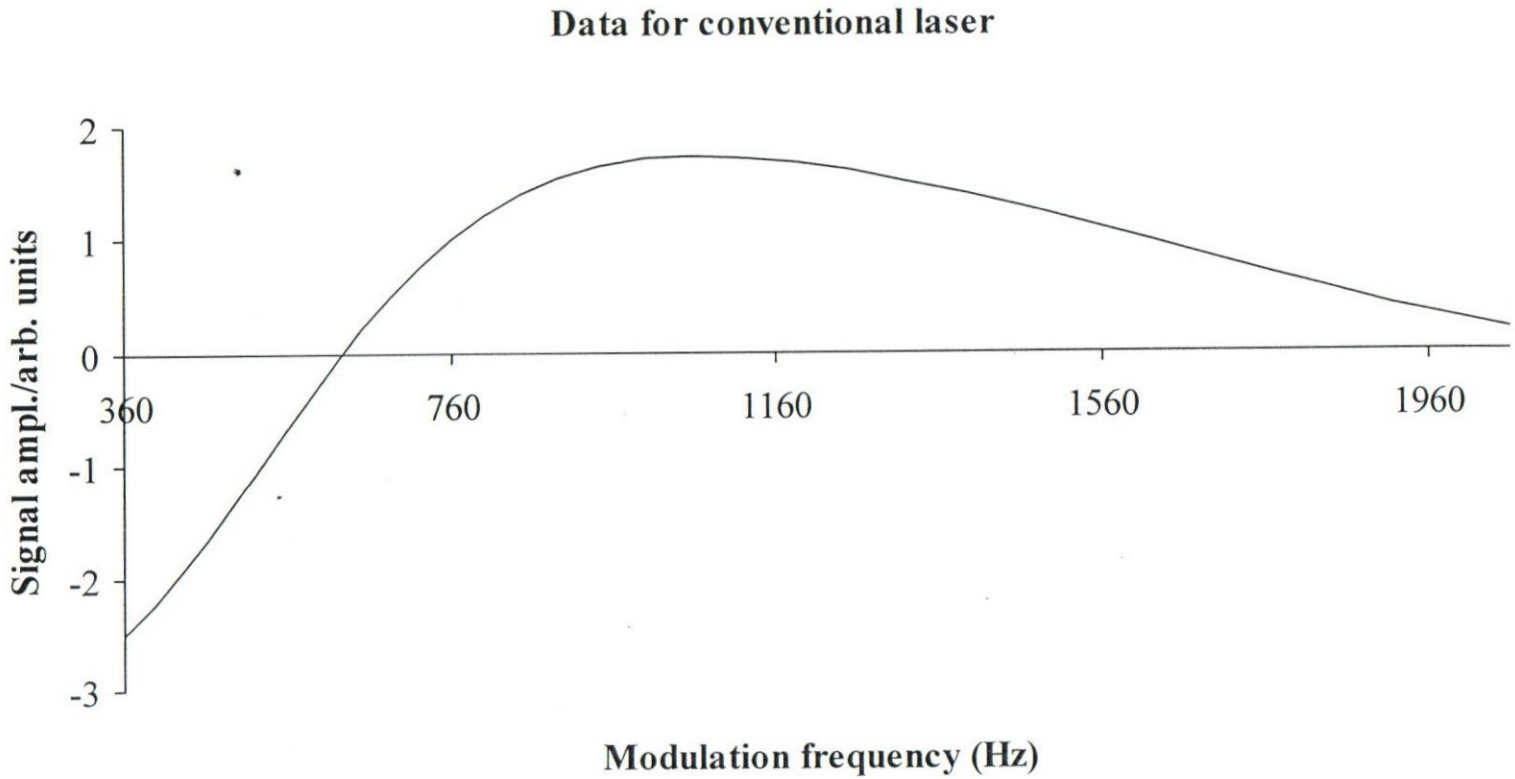

Fig. 4-8: PA signal versus modulation frequency at constant pressure of 16 torr and at a current of 12mA.

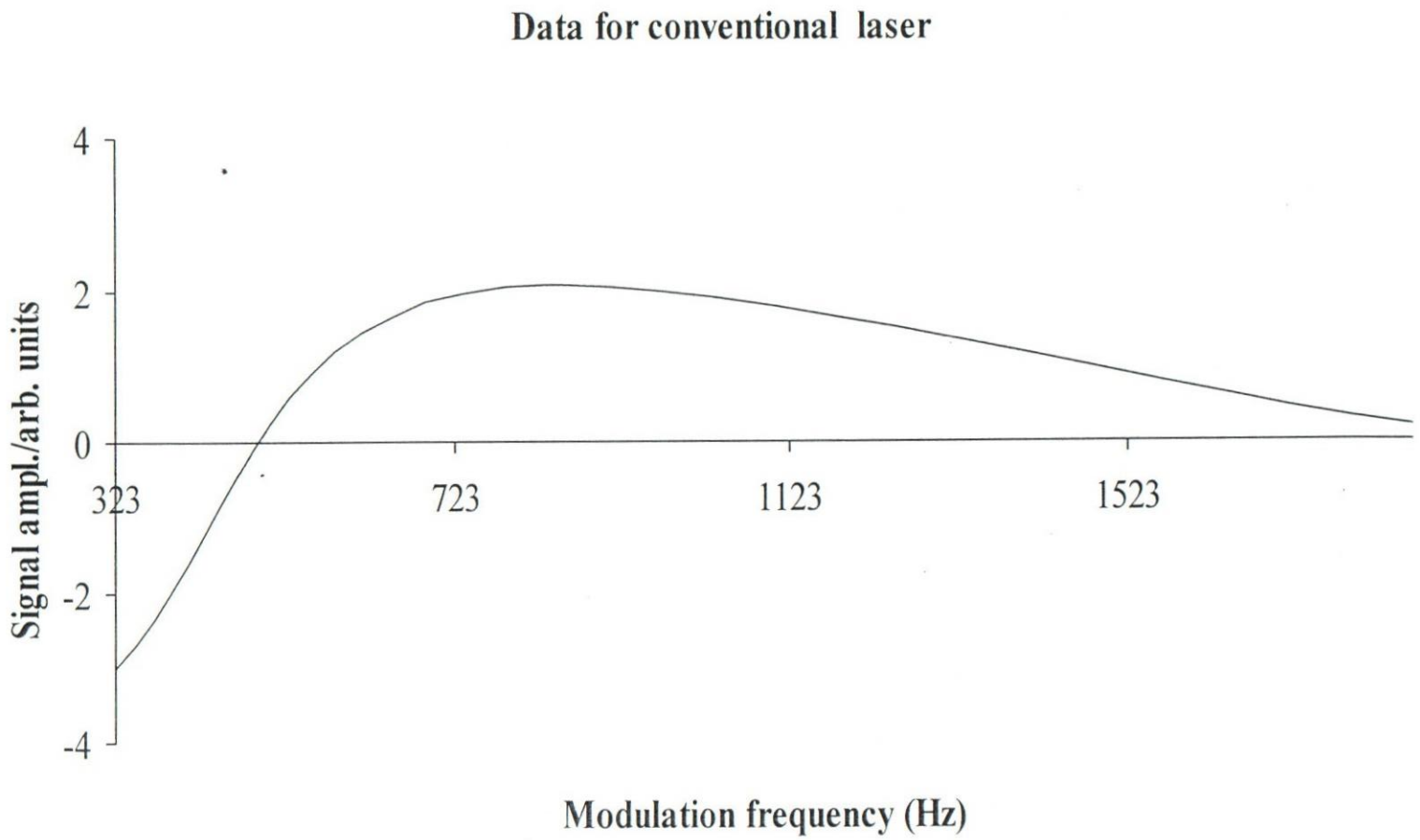

Fig. 4-9: PA signal versus modulation frequency at constant pressure of 18 torr and at a current of 12mA.

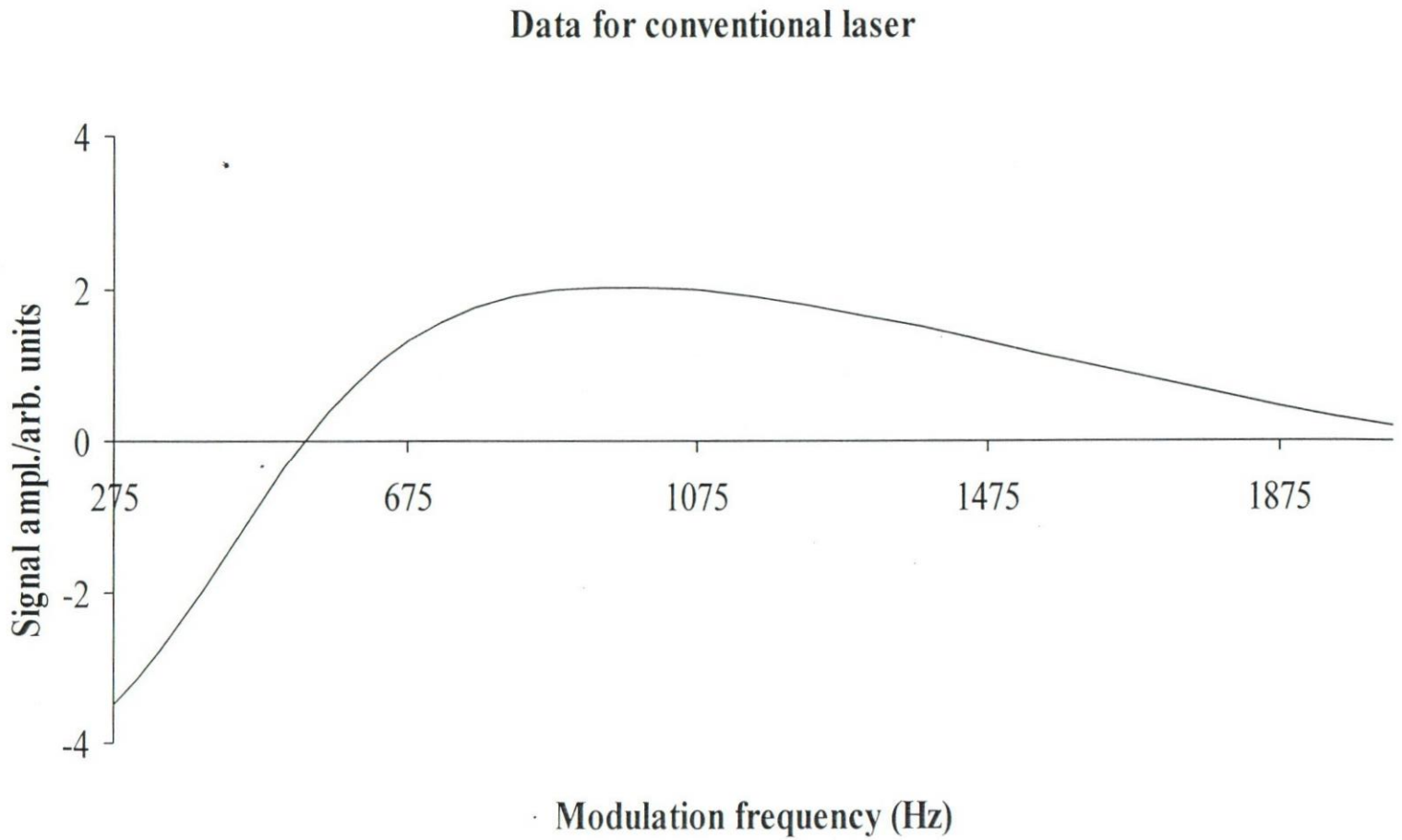

Fig. 4-10: PA signal versus modulation frequency at constant pressure of 20 torr and a current of 12 mA.

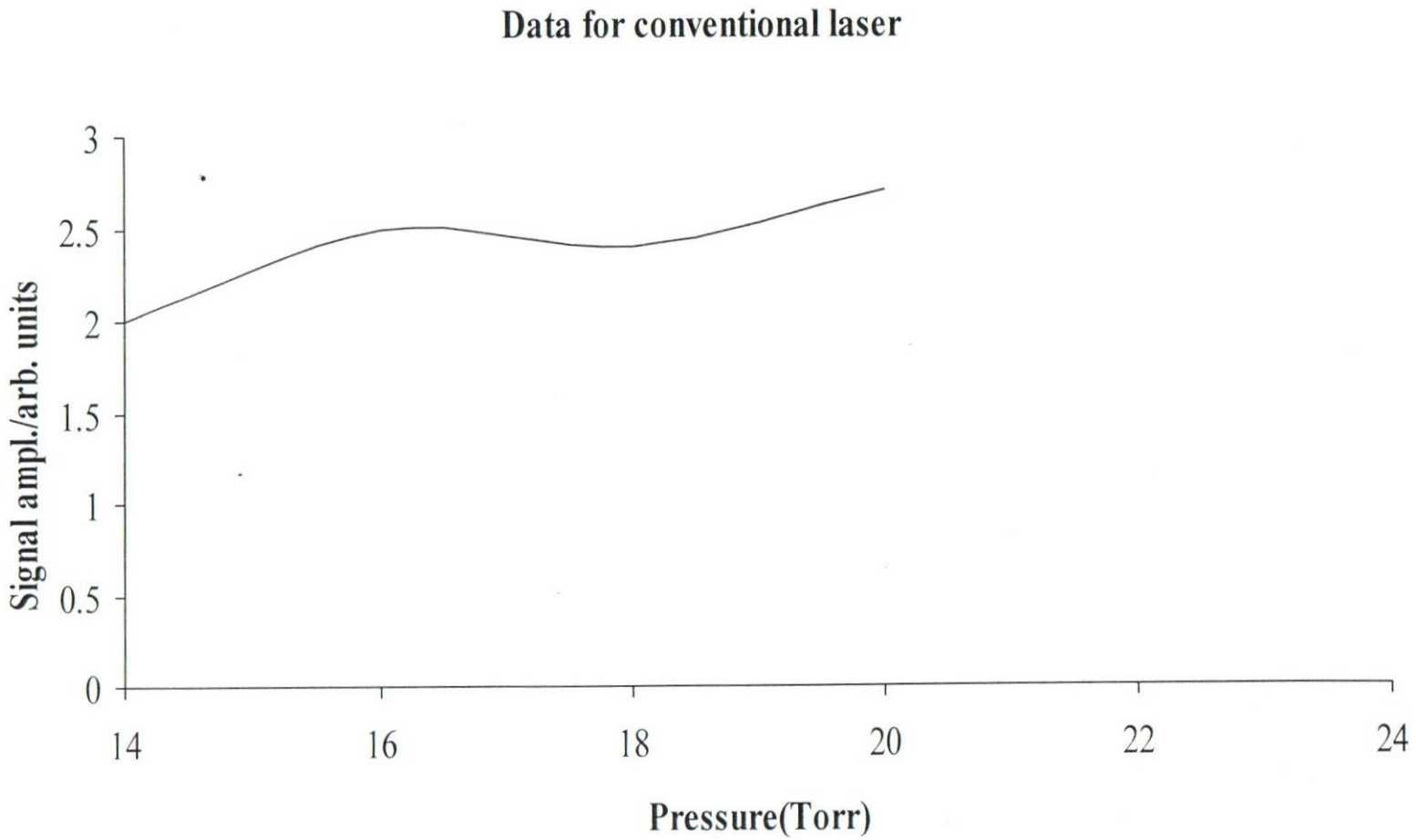

Fig. 4-11a: PA Signal versus pressure at constant frequency of 360 Hz and a current of 12 mA.

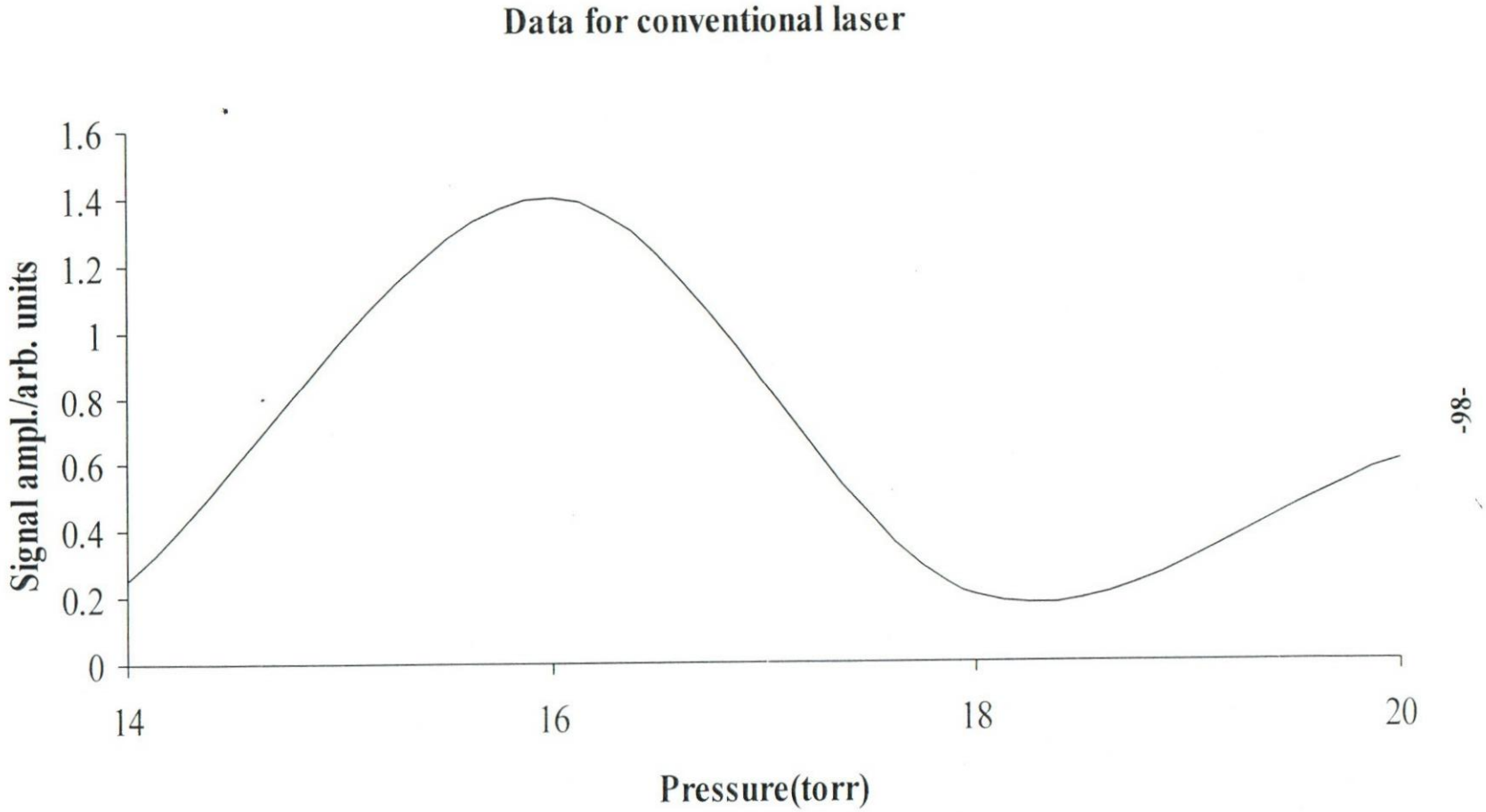

Fig. 4-11b: PA signal versus pressure at constant frequency of 942 Hz and a current of 12 mA.

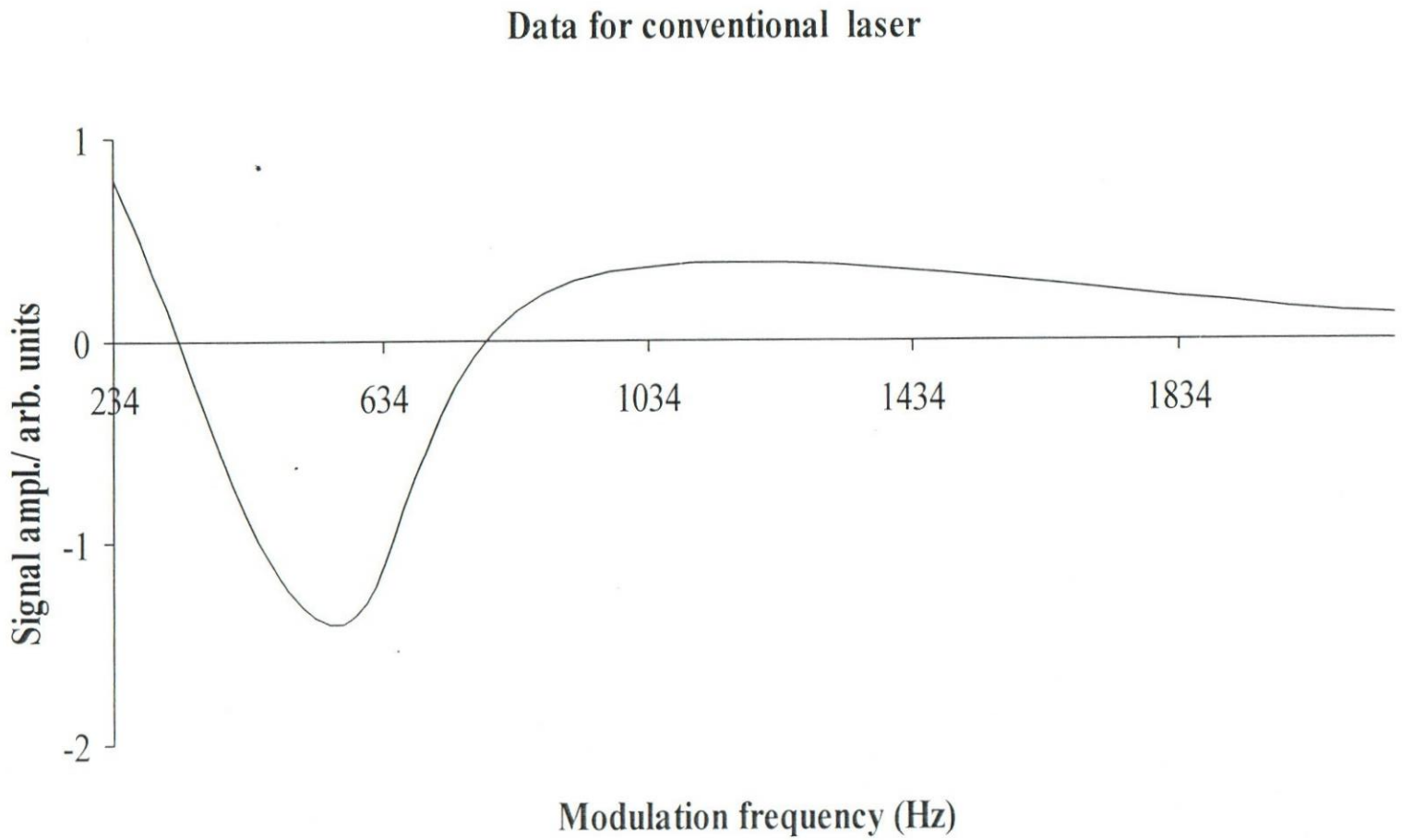

Fig. 4-12: PA signal versus modulation frequency at constant current of 12 mA, and a pressure of 18 torr.

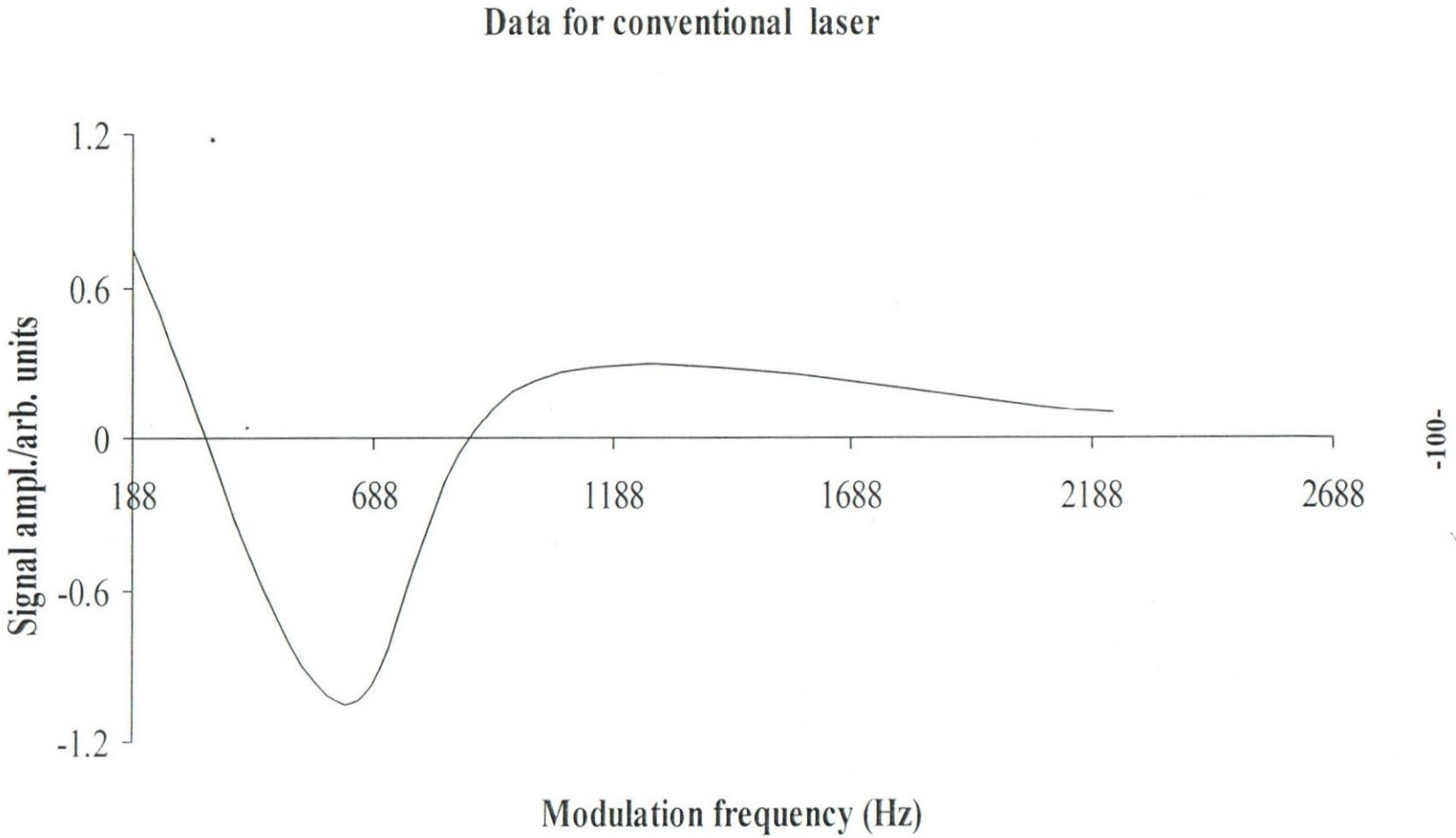

Fig. 4-13: PA signal versus modulation frequency at constant current of 16 mA, and a pressure of 18 torr.

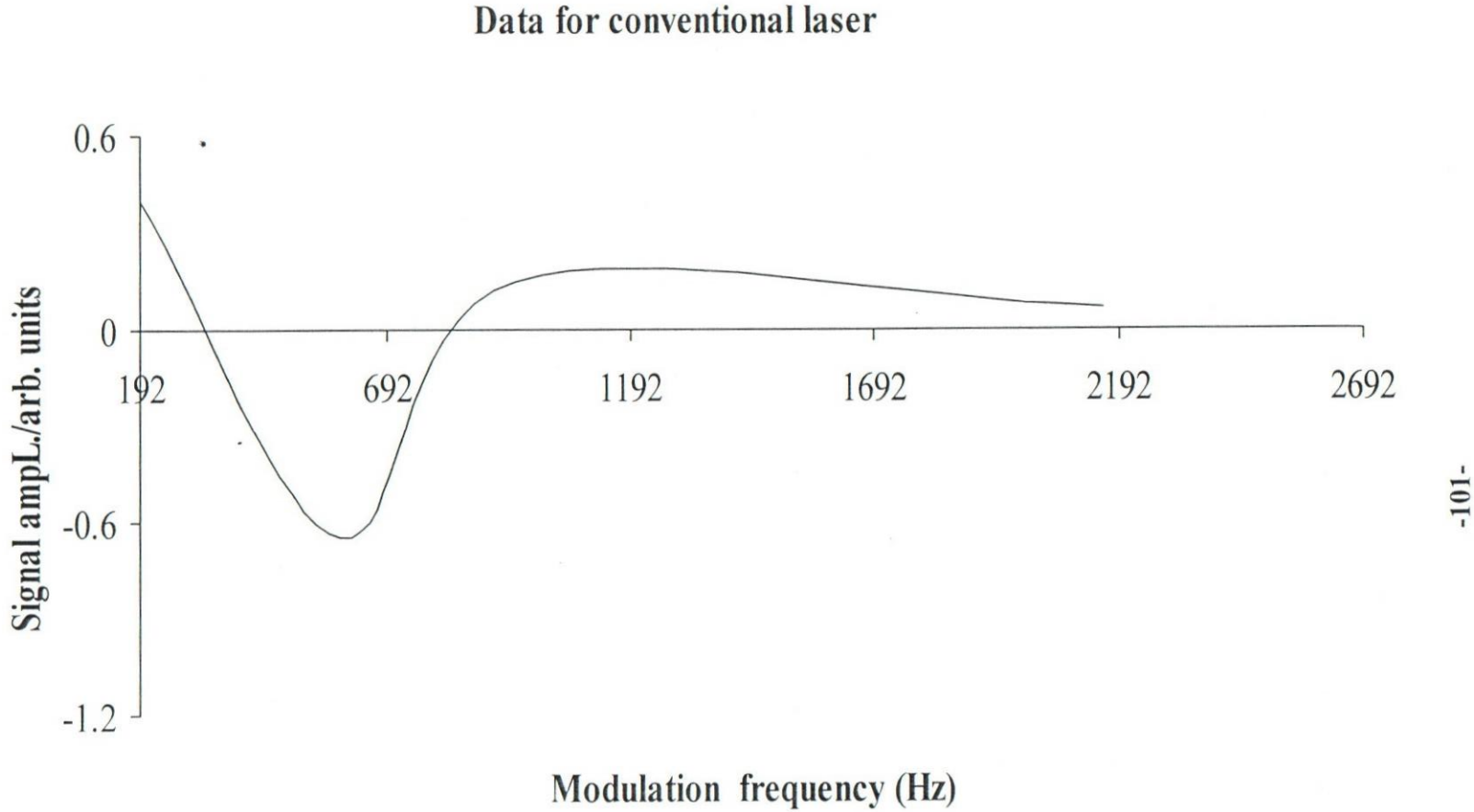

Fig. 4-14: PA signal versus modulation frequency at constant current of 20 mA, and a pressure of 18 torr.

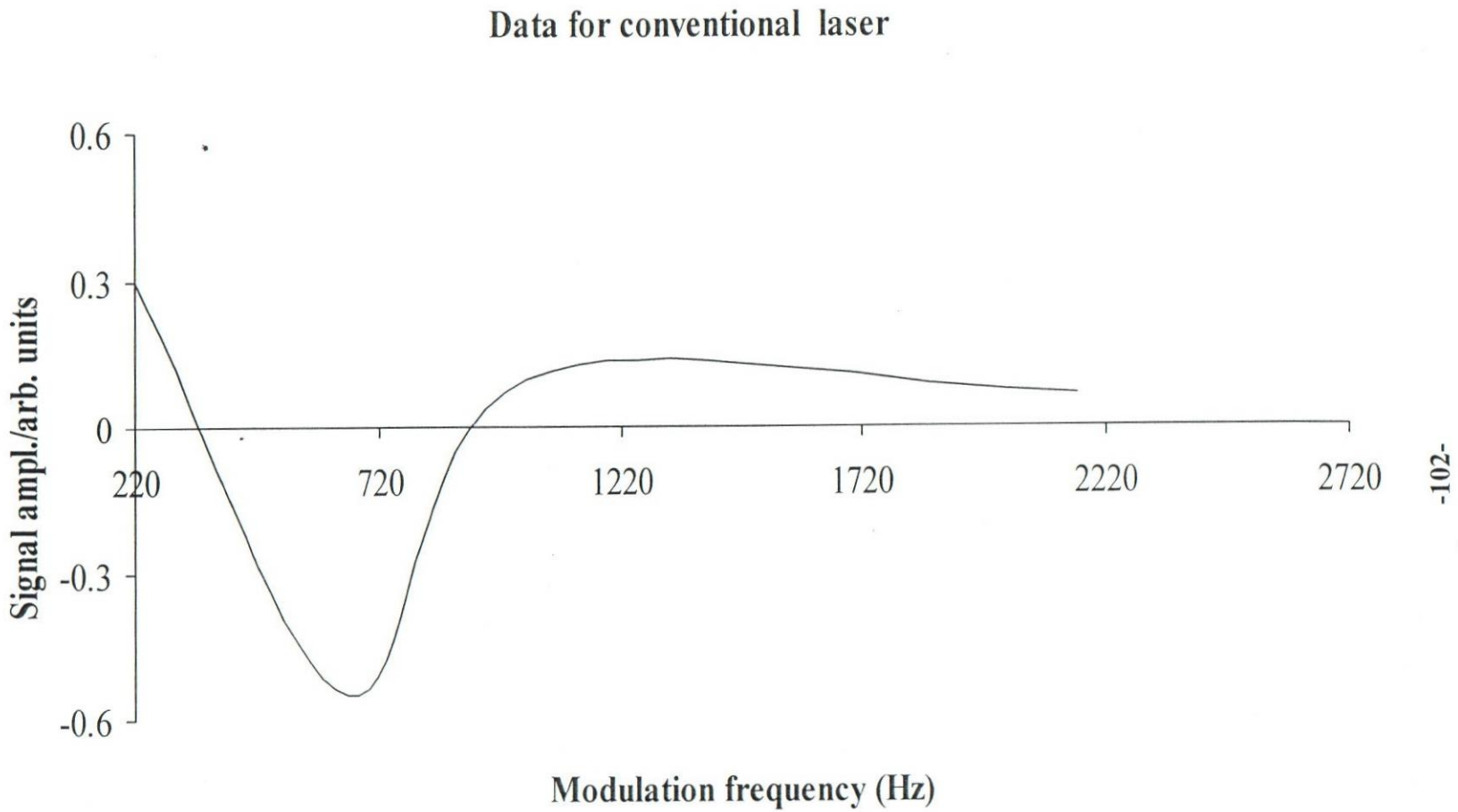

Fig. 4-15: PA signal versus modulation frequency at constant current of 24 mA, and a pressure of 18 torr.

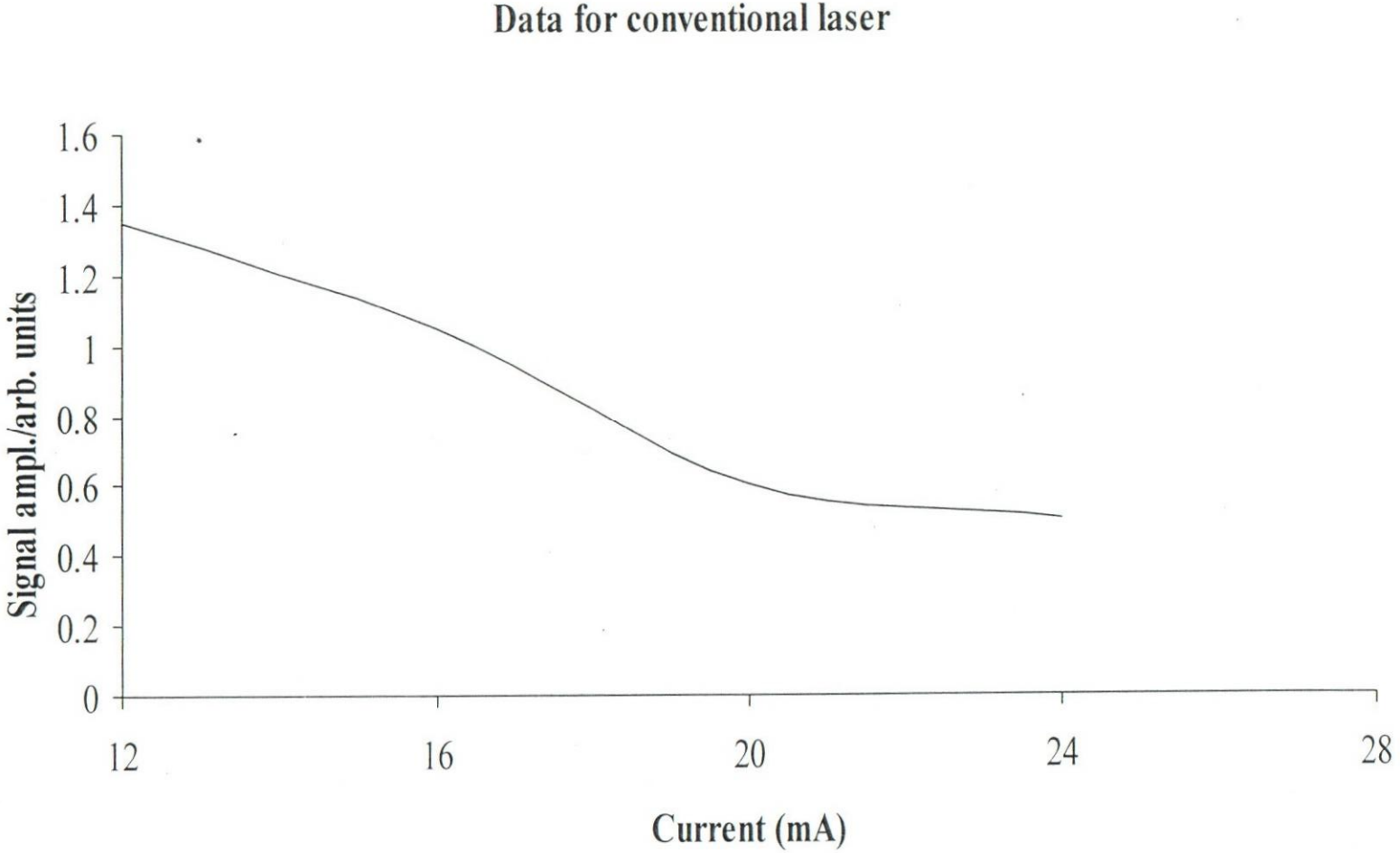

Fig. 4-16a Signal versus current at constant frequency of 620 Hz and at a pressure of 18 torr.

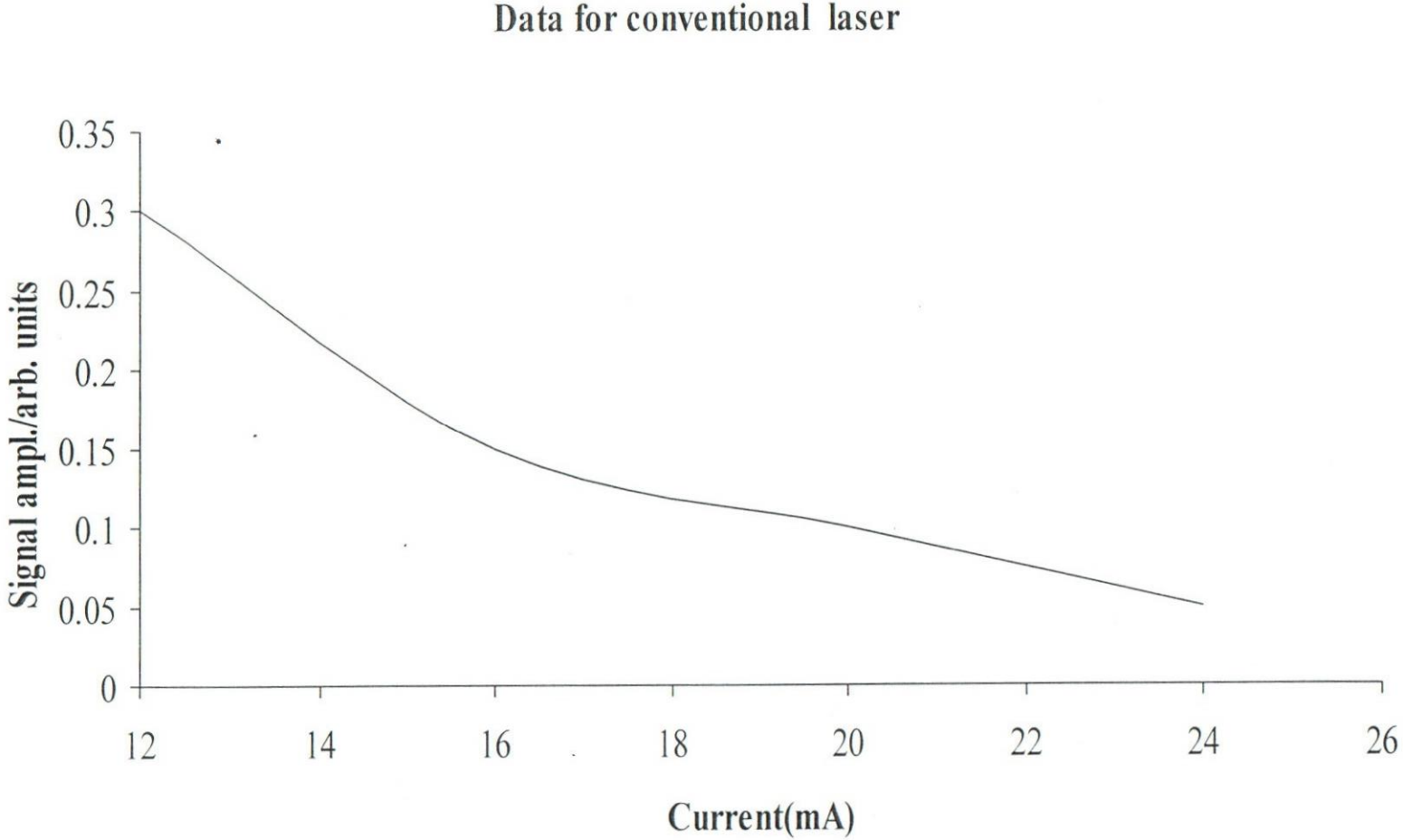

Fig. 4-16b: PA signal versus current at constant frequency of 925 Hz, and at a pressure of 18 torr.

Chapter 5

Discussion

The study presented in this thesis is the first of its kind that compares between PA signals detected in both a conventional and waveguide lasers. Understanding the origin of the PA signals in the laser cavity has many advantages; namely it constitutes a reference of the stability of laser cavity, hence can be used for laser stabilization. PA effect as explained earlier has strong relation with dexcitation of excited atomic species, therefore it can be used as a mean to understand what is going on in the laser cavity, i.e the physical processes that take place. This has its importance on the performance of the laser in general.

The PA signals available for the waveguide and conventional lasers are both detected outside the discharge region, no results to our knowledge is detected in the discharge region. For the conventional laser PA signals were detected for different modulation frequencies, at different pressures and currents. In contrast for the waveguide laser, the study is carried out for different modulation frequencies only, but from different positions in the vicinity of the discharge region and a way from it.

PA signal are generated as a result of excitation and dexcitation of atomic species upon absorption of photons, hence forming an oscillating source of pressure or sound that can be detected using a sensitive

microphone. The level of detected sound signals depends on the level of absorption of light power, the photoacoustic cell design and the modulation frequency. If the cell is designed for resonance action then the signal amplitude is enhanced to the maximum. PA signal level depends also on the number of atomic species being de-excited non-radiatively. The laser cavity is considered a complicated PA cell, since it has no uniform shape. One crucial factor for calculating the theoretical resonance frequencies is the cell volume. The exact volume of the cavity unfortunately cannot be determined due to many ports and pipes connected to cavity for gas inlet, outlet and pressure gauges. It is possible to consider the tubes as separate cells. One way is to consider laser cavity a complex multi cell, either a double or triple resonance cells.

The result of Parslow for the waveguide cavity were very limited where as that of Abu-Taha for the conventional laser were comprehensive. In the later study many parameters changed, for example current and pressure. These parameters which are kept constant for all the results of Parslow are crucial check of type of process occurring in the laser cavity. Only three curves of the response versus frequency for the three microphones were obtained (see fig. 4.4-4.6). The similarity of the pattern of the signals from three microphones indicates beyond no doubt two important facts. Firstly, the similarity of

frequencies with all ranges low medium and high indicate, they belong to same source, i.e. originates and spreaded in the laser cavity. Secondly, the laser cavity as a whole with its complex nature can be considered a resonant cell. It must be remembered that the PA signal can only be generated in the vicinity of the laser beam, where atomic species can be excited and non radiatively de–excited. It follows that the PA signal is generated in the waveguide and transmitted every where in the cavity and the pipes connected to it even against the gas flow in the cavity. The rest of the results have taken for the conventional laser cavity at different conditions. The set of curves represented by figures 4.7- 4.10 taken at different gas mixture pressures. These curves have the same form. They all start by a negative phase signal and end up with high frequency signals. Signal amplitude goes up as the pressure is raised. The speed of sound is higher as the pressure goes up. This condition reveals the importance of PA signals in laser stabilization, for example laser power tends to increase as pressure goes up i.e. more atomic species available for excitations. If the PA signals go up with pressure, hence it changes as the laser power changes.

If the modulation frequency is kept constant at certain resonance value (see figure.4.11a and 4.11b) and the pressure varied in the range 14- 20 torr a peak signal amplitude was noticed at a pressure of 16 torr for both

resonances of 360 and 942 Hz, except the damped amplitude is well pronounced for the 942 Hz at 18 torr. The serge in the PA signal at a particular pressure can only be attributed to the improvement of resonance conditions of the cell. The set of curves obtained at constant pressure of 18 torr and various sets of currents 12mA-24mA in steps of 4mA, have exactly the same form. They all started with a low resonance frequency and a negative phase signal peak at a medium frequency of 555 Hz at 12 mA and up to a 655 Hz at 24 mA. Phase reversals of signals was not mentioned at all by Parslow, 1993. It can be explained on the basis of change direction of compressions and depression on the microphone diaphragm. The reason behind this change is not well known, but can be related to the start of the acoustic signal and its development in the cell. One point worth mentioning here is that the amplitudes of the signals of frequencies 555, 620, 600, 655 Hertz at the corresponding currents 12, 16, 20 and 24 mA respectively, tend to decrease as the current is increased. When the current is increased usually the active medium in the laser cavity tends to become hotter as a result of increased accelerated electron number, hence more energy is dumped in the cavity. Increasing cavity temperature should result in increased PA signal amplitude, contrary to what is noticed above. This can be explained as follows: As the current is increased efficient excitation of N_2 molecules results in efficient

excitation of CO_2 molecules as well, i.e. less non radiative de-excitation which is the source of vibrating pressure for PA signals. This conclusion also noticed from figure. 4.16a and 4.16b when PA signals detected at fixed frequency and pressure, while the current was varied. The continued decay as current is increased indicates that the major source of PA signal generations is decreasing and this is the non-radiative de-excitation. The similarity of curves for the different conditions in the conventional laser also showed that PA signal is generated in the vicinity of the beam and transmitted, so it can be detected any where in the laser system as far as it has access to the laser active medium container. The range of frequencies obtained from both the conventional and waveguide laser cavities are similar, although the cavities are very different in size and shape. This asserts that shape of cavity is not a key factor for resonances. The existence of low detected frequencies mean that laser stabilization using this technique is possible as shown by Abu- Taha, 1987. The limited parameters used by Parslow do not allow a detailed comparison between both lasers. Anyhow one note is that the best response for a waveguide laser cavity was registered at high frequencies of ~ 1KHz for all three microphones, in comparison with a ~ 0.5 KHz for a conventional laser. Discrepancies between measured and theoretically calculated frequencies is mainly due to many reasons concerned with being unable to assign the exact values of the

parameters involved in the calculation. The cavity volume and speed of sound in the laser gas mixture are the major hurdle in the calculation.

Chapter 6

Conclusions and further work

PA signal depends on the level of absorption of light power, the photoacoustic cell design, modulation frequency and the number of atomic species being de–excited non- radiatively. It follows that the PA signal is generated in the wg and conventional laser cavities transmitted everywhere in the cavity and the pipes connected to it even against the gas flow into the cavity. Laser cavity can be considered a complex cavity that has more than one acoustic resonance depending on the conditions of the cavity. The range of frequencies obtained from both conventional and wg laser cavities are similar, although the cavities are very different in size and shape. The best response for wg laser cavity was registered at high frequencies ~ 1 KHz for all three microphones, in comparison with a ~ 0.5 Hz for a conventional laser. The photoacoustic signal reflects sensitively what is going on in the laser cavity, hence can act as a reference to the stability of the laser cavity.

The present work represents a preliminary study that compares an available data for two different laser cavities. More important point needs investigation, namely the size of acoustic signals in discharge and outside it. This type of study will represent a challenge since a sound sensor durable to the high potential and temperature of the plasma is

required. More precise measurements can be achieved using a sealed off cavity that has an exact volume followed by a study that allow the change of all parameters can lead to comprehensive study.

References

Abrams A., Appl. Phys. Lett. 25, 304 (1974).

Abrams R., (1979). Waveguide gas laser, in Laser Handbook, vol.3, Amsterdam, the Netherlands. North- Holland.

Abrams R., IEEEJ.of Quant. Electron, QE-8, 838. (1972).

Abu- Taha M.I., (1987). Optoacoustic frequency stabilization of a carbon dioxide laser, PhD Thesis, University of Keele, UK.

Apfelberg D.B., (Ed). Atlas of cutaneous laser surgery. New York; Raven Press, 1992.

Abu-Taha M.I., and Laine D.C., patent (Frequency stabilization of a CO_2 laser) USA Pat.No. 235062 (1989), UK Pat.No.8981926-4 (1990) and Canadian, Pat.No.575602 (1990).

Biswas D., Nath A., Nundy V., and Chatterjee V., Prog. Quant. Electron., 14, (1990).

Bloom A., Gas lasers [John Wiley and Sons Inc., 1968, U. S. A].

Bridges T., Burkhardt E. and Smith P., Appl. Phys. Lett. 20 , 403 (1972).

Cherrington C., Laser theory, Oct 1979,p.123.

Chester A., and Abrams R., Appl. Phys. Lett, 21, 576. (1972).

Crafer R., Gibson A., Kent M., and Kimmit M., Brit. Appl. Phys. Ser (2) No. 12, 183 (1969).

Degnan J., Appl. Phys. Lett 11, 1-33. (1976).

Dewey C., Kamm R., and Hackett C., Appl. Phys. Lett., 23,633. (1973).

Duley W., (1976). CO_2 lasers effects and applications. Academic Press, London and New York.

Douglas N.G., Millimeter and submillimetre wavelength laser, Springer, Berlin, 1989.

Harren F., and Reuss J., Spectroscopy photoacoustic, Encylopedia of Appl. physics, Vol. 19, 1997.

Goldan P., and Goto k. J., App1. Phys. 45, 4350 (1974).

Goldsbrough J., Laser Handbook Vo1.1, F., Arecchi and E., Schultz (Eds.), [North Holland publishing company, Holland, 1927] P. 598.

Hall D., Laser advances and applications, B.S., Wherrett (Ed)

[Proc. National Quantum Electronic Conference, 1979, Wiley (1980), U.K.] pp. (19- 24). 54 (7), July 1976.

Hawkes J., Latimer I., Lasers theory and practice , University of Northumbria at Newcastle,1Bruce C., Sojika B., Watkins W., White K. and Derzko Z., Appl. Opt. 15, 2970 (1995).

Henk J., and Bicanic D., Concept design and use of the photoacoustic heat pipe cell, Department of Agricultural Engineering and Physics, laser photoacoustic Laboratory, Appl. Phys. Lett. 55 (15), 9 October 1989.

Hochuli V., and Sciacca T., Jr., IEEE J. Quant. Electron. QE-10 ,239(1974)

Hocker L., Kovacs M., Rodes C., Flynn C., and Javan A., Phys. Rev. Lett, 17,233. (1966).

Howe J., Appl. Phys. Lett. 7, 21 (1965).

Kerr E., and Atwood J., Appl. Opt.7, 915. (1968).

Kreuzer L.,(1977). The physics of signal generation and detection in optoacoustic spectroscopy, Poa Y., (ED.). Academic Press New York.

Lehmann K., Scherer G., and Klemperer W., J. Chem. Phys. 77,2853 (1982)

Lengyel B., Introduction to lasers, (John Wiley 1971, U.S.A.).

Luft K. Z., Tech. Phys. 24,92. (1943).

Manes k., and Seguin H., J. Appl. Phys. 43, 5073 (1972).

Marcatili E., and Schmeltzer R., Bell. Syst. Tech.J.43, 1783. (1964).

Marcatili E., and Schmeltzer R.,. Bell. Syst. Tech. J. 43,5073. (1964).

Moller G., and Ridgen J., Appl. Phys. Lett. 7,247. (1965).

Olafsson, A. J., Henningsen, Infrared Phys. Technol. 6,309. (1995).

Parslow D., (1993), Intracavity Optoacoustic detection in a CO_2 waveguide laser using a Helmholtz cell, PhD Thesis, University of Keel, UK.

Patel C., Phys.Rev.Lett, 12,588. (1964).

Patel C., Scientific. American. August 23-33. (1968).

Pfund A., Science. 90,326. (1939)

Pisarchik A.N., and Kuntsevich B.F, Dynamical features of a pump-switched waveguide CO_2 laser with modulated losses, Infrared physics and Technology 39,271-281. (1998).

Ratz J.L., editor. Laser in cutaneous medicine and surgery, Chicago; year Book Medical, (1995).

Robert H. R., An introduction to acoustic, the city of college of New York, (1951).

Rosencwaig A., Photoacoustics and photoacoustic spectroscopy, (John Wiley and Sons. N.Y.1980).

Rosengren L., Max E. and Eng S., J. Phys. E: Sci. Instrum. 7, 125(1974).

Stefens R. W., and, Bate A. E., Wave motion and sound, Senior Lecturer in Physics, Imperial College of Science and Technology, London, (1955).

Scott M., and Myers G., Appl. Opt. 23, 2874 (1984).

Siegman A., (1986). Lasers. University Science Book. Mill Valley, California, 3.

Sigrist M .W., Opt. Eng. 33 ,1916. (1995).

Smith P., Appl. Phys. Lett, 19, 132- 134. (1971).

Sobolev N., and Sokovikov V., Sov. Phys. USP. 10, 153 (1967).

Svelto O.,. Principles of lasers. Hanna D (Ed), 3 rd ed., Plenum Press, New York and London. (1989)

Taylor R., and Bitterman S., Rev. Mod. Phys. 41, 26. (1969)

Thyagarajan K., and Ghatak, A.K., Laser theory and applications, New York and London, Plenum Press, (1981).

Tychinskii V., Sov. Phys. USP. 10, 131. (1967).

Tychinskii V., Sov. Phys. 10,131. (1967).

Tyte D., J. Phys. E. Sci. Instrum. 3,734. (1970).

Tyte D., J. Phys. E.: Sci. Instrum. 3, 743 (1970).

Verdyen J.,(1995). Laser electronics. Prentice- Hall, Englewood Cliffs, New Jersey.

Virupksha R.K., Photoacoustic spectroscopy, Rev. Sci. Instrum..,William C. Elmore, Physics of Waves, Department of Physics, Swarthmore College, McGraw-Hill Book Company, New York, 1983.

Wilson J., and Hawkes J., (1987). Lasers principles and applications. Prentice- Hall, U. K.

Witteman W., Philips. Res. Reports, 21, 73- 84. (1966).

Wood O. (1974). Proc. IEEE. 62,355.

Zharov, V.P., Letokhov, V.S., Laser optoacoustic spectroscopy, Springier Series in optical Science 37, Berlin Heidelbery. Springer Verlage, (1986).

ملخص

يشتهر ليزر ثاني أكسيد الكربون بالعدد الكبير من الأطوال الموجية التي يعطيـــها. وعليـــه استخدم هذا الجهاز استخدامات عديدة سواء في النواحي العلمية، الصناعية، الزراعية أو الطبية. ويكون الليزر أنفع استخداماً عندما يكون ثابت الذبذبة والقوة. ومن الوسائل التي تستخدم كمرجع لثبات الليزر هو التأثير الصوت ضوئي الذي ينشأ في داخل تجويف الليزر أثناء عمله. وتـــهدف الدراسة الحالية للمقارنة بين رنين الإشارة الصوتضوئية الناتجة في تجويفي ليزر ثاني أكســـيد الكربون العادي من أبحاث أبو طه (1987) وتلك التي حصل عليها بارسلو (1993) لـــ لـــيزر (الموجة المقادة). لقد تم اشتقاق المعطيات من نتائج عملية حصل عليها الباحثان، كمـــا جـــرت محاولات لحساب الرنين في التجويفين الليزرين نظرياً بـــافتراض ســـعات مختلفـــة لتجـــاويف الليزرين وذلك من أجل المقارنة. وقد دلت النتائج التي تم التوصـــل إليـــها علـــى أن الإشـــارة الصوتضوئية تحصل بمحاذاة شعاع الليزر داخل التجويف. وهذه الإشارات تعطـــي معلومـــات فيزيائية هامة عما يدور داخل تجويف الليزر. كما وجد توافق بين النتائج العملية والنظرية فـــي الجهازين بشكل عام، مع وجود اختلافات تقع ضمن الخطأ المعقول في ضوء صعوبة تحديـــد الحجم الحقيقي لتجويف الليزر.